Research Paper

PAIN®

ATF4 inhibits TRPV4 function and controls itch perception in rodents and nonhuman primates

Man-Xiu Xie[a], Jun-Hua Rao[b], Xiao-Yu Tian[c], Jin-Kun Liu[c,d], Xiao Li[e], Zi-Yi Chen[f], Yan Cao[e], An-Nan Chen[f], Hai-Hua Shu[g], Xiao-Long Zhang[c,*]

Abstract

Acute and chronic itch are prevalent and incapacitating, yet the neural mechanisms underlying both acute and chronic itch are just starting to be unraveled. Activated transcription factor 4 (ATF4) belongs to the ATF/CREB transcription factor family and primarily participates in the regulation of gene transcription. Our previous study has demonstrated that ATF4 is expressed in sensory neurons. Nevertheless, the role of ATF4 in itch sensation remains poorly understood. Here, we demonstrate that ATF4 plays a significant role in regulating itch sensation. The absence of ATF4 in dorsal root ganglion (DRG) neurons enhances the itch sensitivity of mice. Overexpression of ATF4 in sensory neurons significantly alleviates the acute and chronic pruritus in mice. Furthermore, ATF4 interacts with the transient receptor potential cation channel subfamily V member 4 (TRPV4) and inhibits its function without altering the expression or membrane trafficking of TRPV4 in sensory neurons. In addition, interference with ATF4 increases the itch sensitivity in nonhuman primates and enhances TRPV4 currents in nonhuman primates DRG neurons; ATF4 and TRPV4 also co-expresses in human sensory neurons. Our data demonstrate that ATF4 controls pruritus by regulating TRPV4 signaling through a nontranscriptional mechanism and identifies a potential new strategy for the treatment of pathological pruritus.

Keywords: Acute itch, Chronic itch, Activated transcription factor 4, TRPV4, Dorsal root ganglion

1. Introduction

Activated transcription factor 4 (ATF4), which is also known as cAMP response element binding protein 2 (CREB-2), belongs to the ATF/CREB transcription factor family.[32] It features a basic leucine zipper (bZIP)-type DNA binding domain, which plays a pivotal role in governing gene transcription related to metabolism and apoptosis.[23,24,51,63] Several lines of research have reported that ATF4 plays an important role in various tissues. For example, mice lacking ATF4 expression demonstrate skeletal and lens hypoplasia.[17,57] In the nervous system, the absence of ATF4 has been found to hinder synaptic plasticity and memory formation in hippocampal neurons.[8,12] ATF4 in the suprachiasmatic nucleus of the hypothalamus plays a role in the regulation of biological rhythms.[49] We recently demonstrated that primary sensory neurons within the dorsal root ganglion (DRG) express ATF4 and play a role in regulating thermal nociception.[64] However, whether ATF4 is necessary for itch remains poorly understood.

Specialized membrane proteins in neurons are sensitive to specific stimuli, facilitating the transduction of somatosensory signals. Transient receptor potential channels (TRPs) play crucial roles in transmitting a diverse array of somatosensory stimuli, encompassing itch, pain, temperature, and mechanosensation.[4–6,10] Among these proteins, transient receptor potential cation channel subfamily V member 4 (TRPV4) is a nonselective cation channel expressed in DRG neurons and plays a role in the perception of itching signals.[1,33] Study shows that deletion of TRPV4 significantly inhibits the acute itch behavior induced by histamine and chloroquine (CQ).[33] Mutation of TRPV4 also markedly alleviates chronic pruritus arising from dry skin induced by an acetone/ether mixture followed by water (AEW) and allergic contact dermatitis induced by squaric acid dibutylester (SADBE).[40] Conditional knockout of TRPV4 in DRG neurons of mice reduces compound 48/80- and 5-HT–induced pruritus behavior.[69] Administration of TRPV4 agonist to enhance the function of TRPV4 can induce itching behavior in mice.[67] However, it is still unclear whether ATF4 regulates the TRPV4 channel and is involved in itch modulation.

Here, we reveal a role of ATF4 in itch sensation in mice and nonhuman primates. Activated transcription factor 4 interacts with TRPV4 channels and inhibits the function of TRPV4 through the 117-232 aa fragments in sensory neurons. Thus, our study unveils a novel

Sponsorships or competing interests that may be relevant to content are disclosed at the end of this article.

[a] *Department of Anesthesiology, Sun Yat-sen University Cancer Center, State Key Laboratory of Oncology in South China, Guangdong Provincial Clinical Research Center for Cancer, Guangzhou, China,* [b] *Guangdong Key Laboratory of Animal Conservation and Resource Utilization, Guangdong Public Laboratory of Wild Animal Conservation and Utilization, Institute of Zoology, Guangdong Academy of Sciences, Guangzhou, China,* [c] *Medical Research Institute, Guangdong Provincial People's Hospital (Guangdong Academy of Medical Sciences), Southern Medical University, Guangzhou, China,* [d] *Guangdong Cardiovascular Institute, Guangdong Provincial People's Hospital (Guangdong Academy of Medical Sciences), Guangzhou, China,* [e] *College of Food Science and Technology, Hainan University, Haikou, China,* [f] *Zhongshan School of Medicine of Sun Yat-sen University, Guangzhou, China,* [g] *Department of Anesthesiology, Guangdong Provincial People's Hospital (Guangdong Academy of Medical Sciences), Southern Medical University, Guangzhou, China*

**Corresponding author. Address: Medical Research Institute, Guangdong Provincial People's Hospital (Guangdong Academy of Medical Sciences), Southern Medical University, 106 Zhongshan Rd 2, Guangzhou 510080, China. Tel.: 0086-20-83827812-51151. E-mail address: zhangxiaolong@gdph.org.cn (X.-L. Zhang).*

Supplemental digital content is available for this article. Direct URL citations appear in the printed text and are provided in the HTML and PDF versions of this article on the journal's Web site (www.painjournalonline.com).

PAIN 00 (2024) 1–20

http://dx.doi.org/10.1097/j.pain.0000000000003189

role of ATF4 in the regulation of itch sensation and identifies a potential new strategy for the treatment of pathological pruritus.

2. Methods

2.1. Animals/mice

C57BL/6 mice were procured from the Institute of Experimental Animals at the Sun Yat-sen University, whereas *Atf4*$^{+/-}$ mice on the C57BL/6 background were acquired from Cyagen Biosciences Inc. All animals were housed in cages with temperature maintenance (24 ± 1°C), humidity control (50%-60%), and subjected to a 12/12-hour light/dark cycle. The mice were provided with ad libitum access to water and standard laboratory food. All animal experimental procedures were carried out in compliance with the National Institutes of Health guidelines for animal care and ethics,[71] and they received approval from the Research Ethics Committee of Guangdong Provincial People's Hospital, Guangdong Academy of Medical Sciences. All animals were randomly divided into different experimental or control groups. During the experiments, we found that sex did not affect the regulatory effect of ATF4 on pruritus, so the male C57BL/6 mice were used for the experiments. In the ATF4-knockout-related experiments, both the male and female *Atf4*$^{+/-}$ and littermate wild-type (WT) mice were used. In our study, we used 5- to 6-week-old mice for the electrophysiological experiments and 8- to 12-week-old mice for other experiments.

2.2. Animals/monkey

Six adult male cynomolgus monkeys (Macaca fascicularis) were sourced from Guangzhou Xiangguan Biotechnology Co Ltd in Guangzhou, China and were housed in a nonhuman primates (NHP) experimental facility accredited by the Association for Assessment and Accreditation of Laboratory Animal Care International. The animals were individually housed in rooms with controlled temperature and humidity, and they were maintained on a 12-hour light and 12-hour dark cycle. Before the behavioral assay, all monkeys had undergone a period of acclimatization. All animal care and experimental procedures were conducted in accordance with the Guide for the Care and Use of Laboratory Animals standards adopted by the NIH and approved by the Research Ethics Committee of Guangdong Provincial People's Hospital, Guangdong Academy of Medical Sciences, and Laboratory Animal Ethics Committee of Institute of Zoology, Guangdong Academy of Sciences.

2.3. Immunohistochemistry

Mice and monkey DRGs were harvested and postfixed in 4% PFA for 1hour. Human DRGs and dorsal roots were collected from 3 patient donors (2 male and 1 female) at the Sun Yat-sen University Cancer Center, and informed written consent from all participants or next of kin was obtained before the research. The study was approved by the Research Ethics Committee of the Sun Yat-sen University Cancer Center and Research Ethics Committee of Guangdong Provincial People's Hospital, Guangdong Academy of Medical Sciences. Each donor was undergoing spinal surgery for disease treatment wherein the DRGs were to be sacrificed as the standard of care, and the DRGs and the attached dorsal roots were immediately postfixed in 4% paraformaldehyde. Next, dehydrate the DRG tissue and embed the dehydrated tissue for cryostat sectioning. Incubate the sections with primary antibodies against ATF4 (Mouse, 1:20, Fine test, Boulder, CO, #Fnab00663), TRPV1 (Rabbit, 1:200, Alomone, Jerusalem, Israel, #ACC-030), TRPA1 (Rabbit, 1:200, Abclone, Wuhan, Hubei, China, #A12544), and TRPV4 (Rabbit, 1:200, Alomone, Jerusalem, Israel, #ACC-034) at 4°C overnight. Then, incubate the DRG with secondary antibodies (1:400) including Cy3 donkey antirabbit (IHC, Jackson, West Grove, PA, 711-165-152), Cy3 donkey antimouse (IHC, Jackson, West Grove, PA, 715-165-150), FITC donkey antirabbit (IHC, Jackson, West Grove, PA, 711-095-152), and FITC donkey antimouse (IHC, Jackson, West Grove, PA, 715-095-150) for 1hour at room temperature (RT). Super-resolution images were taken using structural illumination microscope with N-SIM systems (Nikon, Tokyo, Japan).

2.4. In situ hybridization

Reagents, *Atf4*, *Mrgpra3*, *and H1R* probe were purchased from GenePharma. Drop 100 μL of buffer B onto frozen slices and incubate at RT for 15 minutes. Discard buffer B and wash slices with PBS twice (5 minutes each time). Add 100-μL working solution of protease K (prewarmed to 37°C) to each slice and incubate at 37°C for 20 minutes. Next, add 100-μL 2x buffer C to rinse the slices for 3 times (RT). Dehydrate slices by gradient alcohol 70%, 80%, 90%, and 100% (2 minutes each), then dry it in air. Add 100 μL of denaturing solution (prewarmed to 78°C) to each slice and incubate for 8 minutes. After that, dehydrate slices by gradient alcohol 70%, 80%, 90%, and 100% again (2 minutes each, dry in air). Add 100 μL of probe mixture (denatured at 73°C for 5 minutes, 2 μM probe in buffer E) to each slice, then cover it with a coverslip and seal the slices with sealing glue. Incubate slices at 37°C for 12 to 16 hours in situ hybridization apparatus with keeping humidity to prevent drying. Gently remove the cover slide and discard the hybrid solution (denatured probe mixture). Add 100-μL washing solution (prewarmed to 43°C) to each slice at 43°C for 15 minutes. Afterward, add 100 μL of 2x buffer C (prewarmed to 37°C) to each section and wash twice (10 minutes for each time). Then, wash with PBS for 10 minutes one time. Add 10-μL Dapi Fluoromount-G, cover with a coverslip, and observe with a fluorescence microscope.

2.5. Western blotting

The DRGs were dissected and then dissolved in cold RIPA buffer. A protein extraction kit (Invent Biotechnologies, #SM-005) was employed to separate and isolate the membrane and cytoplasmic proteins.[64] Samples were separated through gel electrophoresis and then, the PVDF membrane was incubated with primary antibodies against ATF4 (Rabbit, 1:1000, Cell Signaling Technology, Danvers, MA, #11815S), TRPV4 (Rabbit, 1:200, Alomone, Jerusalem, Israel, #ACC-034), TRPV1 (Rabbit, 1:200, Alomone, Jerusalem, Israel, #ACC-030), TRPA1 (Rabbit, 1:1000, Abclone, Wuhan, Hubei, China, #A12544), TfR (Mouse, 1:1000, Thermo Fisher Scientific, Waltham, MA, #13-6800), β-actin (Mouse, 1:2000, Affinity, Changzhou, Jiangsu, China, #T0022), β-tubulin (Mouse, 1:2000, Arigo, Hsinchu, Taiwan, China, #ARG62347), Flag-tag (Rabbit, 1:1000, Cell Signaling Technology, Danvers, MA, #14793), or His-tag (Rabbit, 1:1000, Cell Signaling Technology, Danvers, MA, #12698) overnight at 4°C. Then, it was incubated with secondary antibodies (1:10,000), including peroxidase-labeled goat antirabbit (WB, SeraCare, Milford, MA, 074-1506) and peroxidase-labeled goat antimouse (WB, SeraCare, Milford, MA, 074-1806) and then detected the immunocomplexes.

2.6. Qualitative Polymerase Chain Reaction (Q-PCR)

The RNA extraction kit (9767, TaKaRa, Tokyo, Japan) was used to extract total RNA from mouse DRG. According to the manufacturer's protocol, reverse transcription was performed using

PrimeScript RT Master Mix (Perfect Real Time) (RR036Q, TaKaRa, Tokyo, Japan). The primer sequences used are listed here: *H1R*-F, 5′-GGGAAAGGGAAACAGTCACA-3′, *H1R*-R, 5′- ACTGTCGAT CCACCAAGGTC-3′; *H4R*-F, 5′-TGCTCTTGGAATTCCTGCTT-3′, *H4R*-R, 5′-CCAGAAGGAACCCACTTTGA-3′; *MrgprA3*-F, 5′- ACA CAAGCCAGCAAGCTACA-3′, *MrgprA3*-R, 5′- ACTTCCAGGGAT GGTTTCGT-3′; *GAPDH*-F, 5′-CCCATTCTTCCACCTTTGAT-3′, *GAPDH*-R, 5′-CAACTGAGGGCCTCTCTCTT-3′. Quantitative real-time PCR was performed using TB Green Premix Ex Taq II (Tli RNaseH Plus) (RR820A, TaKaRa, Tokyo, Japan) and the CFX96 Touch Real-Time PCR Detection System. The reactions were set up according to the manufacturer's instructions. PCR conditions involved incubation at 95°C for 30 seconds, followed by 40 cycles (95°C for 5 seconds, 60°C for 30 seconds). The relative expression levels of mRNA were determined using the $2^{-\Delta\Delta CT}$ method.

2.7. Coimmunoprecipitation

Transfected HEK293T cells or DRG tissues were lysed using cold Co-IP RIPA buffer. The lysates were subsequently subjected to centrifugation at 14,000g for 15 minutes, with 5% of each supernatant being set aside for the input sample. The remaining supernatant was subjected to an overnight incubation at 4°C with 5 to 10 μg of ATF4 antibody (Cell Signaling Technology, Danvers, MA, #11815S) or His antibody (Cell Signaling Technology, Danvers, MA, #12698). Following this incubation, protein A/G beads (GE Healthcare, Little Chalfont, Buckinghamshire, United Kingdom) were added, and the mixture was further incubated at 4°C for 4 hours. The immunoprecipitated samples were then denatured and prepared for subsequent immunoblotting analysis. Immunoprecipitation was carried out using antibodies specific to TRPV4, TRPV1, TRPA1, ATF4, Flag-tag, or His-tag.

2.8. Proximity ligation assay

Proximity ligation assay (PLA) was performed using Duolink reagents (Sigma-Aldrich, St. Louis, MO, #DUO92101) on cultured mouse DRG neurons.[61] The isolated DRG neurons were cultured according to the method provided below. After 2 days of culture, the cells were fixed with 4% paraformaldehyde at room temperature for 15 minutes and permeabilizated with 0.1% Triton X-100 for 30 minutes. Proximity ligation assay was performed under the Duolink PLA Protocol of Sigma-Aldrich to examine the interactions between the proteins. Briefly, cells on coverslips were blocked with Duolink Blocking solution and incubated with a mixture of 2 primary antibodies ATF4 (Mouse, 1: 20, Fine test, Boulder, CO, #Fnab00663) and TRPV4 (Rabbit, 1: 200, Alomone, Jerusalem, Israel, #ACC-034) overnight at 4°C. After incubation, the coverslips were washed with wash buffer A and then incubated with secondary antibodies (anti-mouse MINUS probe and anti-rabbit PLUS probe) for 1 hour at 37°C. Coverslips were then washed and incubated with PLA ligase. They were subsequently exposed to the polymerase in amplification buffer for 100 minutes at 37°C. The coverslips were then mounted in a mounting medium that contained DAPI, and images were captured using a microscope. In addition, a negative control test was performed by omitting the primary antibody.

2.9. Microinjection of adenoassociated virus into the cervical spinal nerves

According to previous study,[31] mice were anesthetized with isoflurane (4% for induction and 1.5%-2% for maintenance), and then, the nape of the neck was shaved. After the skin was incised, the muscle on C3 to C5 vertebrae was opened with a retractor. For microinjection into the cervical spinal nerves of the DRGs (C3 and C4), we carefully removed the muscle covering the cervical spinal nerves. The glass microcapillary was inserted directly into the spinal nerves just distal to the left cervical DRGs (C3 and C4). The unilateral injection (left side) was to minimize the time and tissue damage related to the operation. The adenoassociated virus (AAV, serotype 5, 5.9×10^{12} vg/mL) of rAAV-hSyn-*Atf*4-2A-enhanced green fluorescent protein (EGFP) was obtained from BrainVTA Biotechnology, and AAV solution was pressure ejected (100 nL/minute) for 3 minutes (300 nL in spinal nerve) using the Micro Syringe Pumps. After microinjection, the inserted glass microcapillary was removed from the spinal nerve, the skin was sutured with 3-0 silk, and mice were kept on a heating light until recovery. Three weeks later, these mice were used for all experiments.

2.10. Intrathecal small interfering RNA (siRNA) and adenoassociated virus injection

Intrathecal administration was conducted using a polythylene-10 catheter as previous,[64] which was placed into the subarachnoid space of mice through the L5 to L6 intervertebral spaces, with the tip of the catheter at the L5 level, and 10 μL of reagent was injected into the cerebrospinal fluid. Inject a mixture of 10-μg siRNA (catalog: L-042,737-01-0020, Dharmacon) and 7.5-μg transfection reagent (chimeric rabies virus glycoprotein fragment, RVG-9R, Anaspec, Fremont, CA) in 10 μL D5W (dextrose 5% in water) into the subarachnoid space 48 hours before the experiments. The experiments were conducted 21 days after intrathecal injection of rAAV-hSyn-*Atf*4-2A-EGFP, rAAV-hSyn-*Atf4*-ΔbZIP-2A-EGFP, rAAV-hSyn-*Atf4-His (117-232)*-2A-EGFP (BrainVTA, 10 μL, serotype 5, 2.0×10^{12} vg/mL), and rAAV-CAG-*GCaMp6s* (BrainVTA, 10 μL, serotype 9, 2.0×10^{12} vg/mL).

2.11. Mouse acute itch models and behavior test

Before conducting the tests, the back of the necks of the mice were shaved. The mice were habituated to the testing environment daily for 2 days before the tests. We administered a 50 μL of intradermal injection of pruritic agents at the nape of the neck and systematically recorded scratching behavior through video monitoring for a duration of 30 minutes, ensuring that no human observers were present to minimize potential interference or bias. We considered a scratch to have occurred when a mouse raised its hind paw to scratch the shaved area and then subsequently lowered the paw either to the floor or toward its mouth for licking. The following doses for pruritic agents were chosen: 100 μg for histamine (2 μg/μL, dissolved in saline), 200 μg for chloroquine (CQ, 4 μg/μL, dissolved in saline), and 50 μg for SLIGRL (1 μg/μL, dissolved in saline). The histamine and CQ were purchased from Sigma-Aldrich, and SLIGRL was purchased from MCE. We reviewed the recorded videos offline and quantified the number of scratching episodes using a blind method. For antagonist experiments, the TRPV4 antagonist 2-Methyl-1-[3-(4-morpholinyl)propyl]-5-phenyl-N-[3-(trifluoromethyl)phenyl]-1H-pyrrole-3-carboxamide HC 067,047 (HC; Tocris Bioscience, Bristol, United Kingdom) was initially dissolved in 100% DMSO and then diluted with saline. HC (10 mg/kg) was administered intraperitoneally to mice, and its effects on itching were observed.

2.12. Mouse chronic itch model and behavior test

Mice were habituated to testing environment daily for 2 days before tests. To induce contact dermatitis chronic pruritus, we applied 0.2 mL of 1% diphenylcyclopropenone (DCP, dissolved in acetone,

purchased from ACMEC, # D88000-5g) on the back of the neck for sensitization. Seven days after sensitization, we applied 0.2 mL of 0.5% DCP to the skin on the back of the neck of mice on days 1, 4, 7, 10, and 14. After application of DCP, we recorded the scratching behavior of mice for 60 minutes. To induce chronic pruritus-associated allergic contact dermatitis, we applied 0.2 mL of 0.5% DNFB (Sigma-Aldrich, St. Louis, MO) in acetone to the back of the neck for sensitization on day 1. Following sensitization, 0.2 mL of 0.25% DNFB was applied to the skin on the back of the neck of mice on days 5, 7, 9, and 11. On day 12, we recorded the scratching behavior of mice for 60 minutes.

2.13. Mechanical itch test

To test the mechanical itch, the fur on the nape of the neck was shaved. Mice were acclimated in a recording chamber with a removable mesh cover for at least 3 days. Mechanical stimuli were delivered with von Frey filaments ranging from 0.02 g to 0.6 g. Mechanical stimulation was applied and continued for 5 seconds unless the mouse responded. The 5 stimuli were evenly distributed on both sides of the body axis. The total number of positive responses elicited by the 5 stimuli were recorded.

2.14. Intrathecal siRNA in the nonhuman primates

The cynomolgus monkeys were anesthetized by intramuscular injection of Zoletil (3-5 mg/kg). Remove the hair on the lower back of the cynomolgus monkeys. Next, place it on the animal operating table and maintain lateral decubitus position. Then disinfect the operative area twice with Anerdian and lay the surgical hole towel. The surgical assistant fixed the cynomolgus monkey's body position so that it can keep a maximal spine flexion. Use the anterior superior iliac spine to locate the L5 spinous process. Hold a 2.5-mL syringe in the right hand and inject the needle into the L4 intervertebral space. In the process of injection, slowly push the needle until there is a sense of breakthrough, then retract needle bolt to see the clear cerebrospinal fluid, and discard the injection tube. We first validated siRNA with monkey derived vero cells and then methylated and cholesterol-modified siRNA for in vivo intrathecal injection (Ribobio, sequence: CAAGCACTTCAAACCTCAT). Use another 2.5-mL syringe to draw 400-μL siRNA mixture (20 nmol siRNA mixed in 400 μL saline) and connect the original injection needle to inject the mixture into the subarachnoid space. Follow the principle of asepsis in the whole process. Behavioral tests were performed 2 days after siRNA injection.

2.15. Nonhuman primates acute itch models and behavior test

The monkeys acclimated to the restraint chair for 1 hour a day for a week before the behavioural tests. We intradermally injected 10 μL of pruritic agents (histamine; 1 μg/μL) into the hindfoot plantar of cynomolgus monkeys to establish the NHPs acute itch models[30] and video recorded scratching behavior for 30 minutes in the absence of any observer. A scratch was counted when a monkey scratched the injected region. We reviewed the recorded videos offline and quantified the number of scratching episodes using a blind method.

2.16. Cell culture and transfection

Mouse DRGs were freed from their connective tissue sheaths and broken into pieces with a pair of sclerotic scissors in DMEM/F12 (Gibco, Grand Island, NY) at a low temperature. After mechanical dissociation, the DRG neurons were subjected to digestion with collagenase (3 mg, Sigma-Aldrich, St. Louis, MO) and trypsin (2 mg, Sigma-Aldrich, St. Louis, MO) for 20 minutes in 5 mL of culture medium. Subsequently, the neurons were plated on glass coverslips coated with poly-L-lysine (Sigma-Aldrich, St. Louis, MO) in a humidified atmosphere (5% CO_2, 37°C). After a period of incubation, follow-up experiments were performed. HEK293T cells were cultured in DMEM with 10% foetal bovine serum. TRPV4-Flag, ATF4-His, and ATF4-His (aa 1-116, 117-232, 233-349) were obtained from Synbio Technologies. The cells were transfected with 1-2 μg of plasmid per 35-mm dish or 2-3 μg of plasmid per 60-mm dish using Lipofectamine 3000 reagent (Invitrogen, Carlsbad, CA). The cells were used for subsequent experiments 24 to 48 hours after transfection.

2.17. Surface protein biotinylation

The expression of plasma membrane proteins was assessed through cell surface biotinylation, using a Cell Surface Protein Isolation Kit (Pierce, #89881), following the manufacturer's instructions. In brief, cells were rinsed with PBS and then biotinylated with Sulfo-NHS-SS-Biotin in PBS for 30 minutes at 4°C. Following quenching, cell lysis was performed, and labeled proteins were extracted by incubating with NeutrAvidin Agarose beads for 60 minutes at room temperature (RT). After thorough washing, the proteins were eluted by heating the beads for 5 minutes at 95°C and prepared for immunoblotting.

2.18. In vitro calcium imaging

Ca^{2+} imaging was conducted in cultured DRGs from WT, *Atf4*$^{+/-}$, and rescue mice after loading cultured DRGs with 3 μL of Fluo-4 diluent (50 μg Fluo-4AM dissolved in 45.6 μL DMSO) for 30 minutes in DMEM/F-12 medium at room temperature (avoid light). Then discard the DMEM/F-12 medium and add the Ca^{2+} imaging buffer for Ca^{2+} imaging. The imaging buffer includes 136 mM NaCl, 1.0 mM $MgCl_2$, 2.0 mM $CaCl_2$, 5.4 mM KCl, 10 mM D-Glucose, 0.33 mM NaH_2PO4, 10 mM HEPES, and pH = 7.4. The fluorescence reflecting the Ca^{2+} signal was imaged in a Laser Scanning Confocal Microscope (Leica SP5-FCS), and calcium flux was analysed from the mean fluorescence measured with LAS AF system. Dorsal root ganglion plates were recorded for more than 7 minutes, which was divided in 1 minute of initial reading (0-s mark, baseline values, F0), followed by stimulation with 2 μL of GSK1016790A (1 μM, TRPV4 agonist), capsaicin (100 nM, TRPV1 agonist), and allyl isothiocyanate (AITC, 200 μM, TRPA1 agonist) at the 120-s mark and 2-μL KCl at the 300-s mark (40 mM). Ca^{2+} signal amplitudes were presented as $\Delta F/F0 = (Ft - F0)/F0$ as ratio of fluorescence difference ($Ft - F0$) to basal value (F0). The average fluorescence intensity of the baseline period was set as F0, and the average fluorescence intensity of the record time (t) was remarked as Ft.

2.19. Electrophysiological recordings

Whole-cell membrane currents of freshly dispersed mouse DRG neurons were performed with an EPC-10 amplifier and PatchMaster software (HEKA Electronics, Lambrecht, Germany). Current was recorded with glass pipette (2-5 MΩ resistance) fabricated from borosilicate glass capillaries using a Sutter P-97 puller (Sutter Instruments, Novato, CA). The pipette solution contained the following (in millimoles): 110 CsCl, 3 $MgCl_2$, 10 EGTA, 10 HEPES, 3 Mg-ATP, 0.6 GTP, and pH 7.2 with CsOH. The extracellular

solution contained the following (in millimoles): 120 NaCl, 5 KCl, 5 $CaCl_2$, 2 $MgCl_2$, 10 glucose, 10 HEPES, and pH 7.4 with NaOH. The osmolality of all solutions was adjusted to 310 mOsm. We administered 4α-Phorbol-12,13-didecanoate, 4-αPDD (10 μM, Sigma-Aldrich, St. Louis, MO) to induce TRPV4 current using a perfusion system and recorded the current after a 10-minute perfusion. The neurons were held at 0 mV to inactivate voltage-gated calcium and sodium channels, and a 150-millisecond linear ramp protocol was applied (−100 mV to +100 mV every 15 seconds). The voltage for current analysis was ±80 mV. Sampling frequency for acquisition was 10 kHz, and data were filtered at 2 kHz.

2.20. In vivo calcium imaging of dorsal root ganglion

The intrathecal tube was inserted into the dura mater to inject 10 μL (BrainVTA, serotype 9, 2.0×10^{12} vg/mL) of rAAV-CAG-*GCaMp6s*. The mice recovered 3 weeks before calcium imaging, as described in previous studies.[13,42] Before imaging, the initial dose of 0.3 mL of urethane (12.5% wt/vol) was intraperitoneally injected. After about 15 minutes, the further doses were titrated to the level of anesthesia until surgical depth was achieved. Use a constant temperature heating pad to maintain the core temperature at about 37°C and observe the temperature through the rectal probe. The skin of mice was prepared, and an incision was made on the skin between L3-L5 spinal segments. Resect the connective tissue and muscle on and around the vertebrae and perform small transverse laminectomy around L4 DRG, with dura mater and perineurium intact. The mice were placed prone on a customized microscope table. The spine is stabilized with custom designed clamps to minimize movement during testing. The mice were imaged under the 25X objective of the Multiphoton Laser Confocal Microscope (FVMPE-RS). We used 10 seconds/frame and 800 × 800-pixel resolution for the L4 DRG. The imaging was monitored during the activation of DRG neuronal soma by the injection of histamine (2 μg/μL, 5 μL) and CQ (4 μg/μL, 5 μL) into the hindpaw, and the laser wavelength was 488 nm. We exported the raw images and used Fiji/ImageJ (National Institutes of Health) to analyze calcium imaging data. The optical planes obtained from consecutive time points were realigned and adjusted for motion using the stackreg rigid-body cross-correlation-based image alignment plugin. The overall count was conducted by employing the thresholding function in ImageJ software from a high-quality, Z stack image of DRG at baseline. The size of activated neurons was determined by using the area function within ImageJ. The raw data were background subtracted and normalized by subtracting the baseline and dividing the difference with the baseline to generate $\Delta F/F_0$, where F_0 is the average fluorescence intensity measured in the baseline period. Regions of interest (ROIs) around neuronal cell bodies were chosen using a free-hand selection tool in Fiji/ImageJ. The ROIs used to determine GCaMP fluorescence were strictly selected to minimize overlap to ensure less interference from surrounding somata. The ROIs used to calculate the neuron cell body size was then selected to be less rigorous, allowing the cells to approach overlapping areas to reflect more accurate cell diameter calculations. Activation of a cell was defined as an increase in fluorescence intensity (ΔF) ≥ 30% of baseline (F_0).

2.21. Data analysis

The grayscale intensities of the western blotting bands were measured using Tanon Gis software. The grayscale values of the images and colocalization were analyzed using Fiji/ImageJ and Image-Pro Plus software. All western blotting, immunostaining, electrophysiological, and behavioral data are presented as the mean ± SEM and were analyzed using GraphPad Prism 9. The threshold for statistical significance was set at $P < 0.05$.

3. Results

3.1. Activated transcription factor 4 is expressed in pruritus-related sensory neurons

To investigate the potential role of ATF4 in itch regulation, we first explored the expression pattern of ATF4 in sensory neurons. The specificity of ATF4 antibody was examined in *Atf4*$^{+/-}$ mouse cervical DRG tissues. The data demonstrated a decrease in ATF4 expression in the DRG tissues of *Atf4*$^{+/-}$ mice (**Figs. 1A and B**), suggesting that the ATF4 antibody is specific. Immunostaining showed that ATF4 was expressed in most sensory neurons (**Fig. 1B**). Size-frequency analysis showed that ATF4 protein was widely expressed in small, medium, and large sensory neurons (Supplementary Fig. 1a, http://links.lww.com/PAIN/C9). Studies have demonstrated that Mas-related GPCR A3-positive (Mrgpra3$^+$) and histamine receptor type 1–positive (H1R$^+$) sensory neurons have been identified as 2 major pruritus-sensing neuronal populations.[7,66] Double fluorescence in *situ hybridization* showed that the mRNA of *Atf4* was expressed in *Mrgpra3*$^+$ and *H1R*$^+$ sensory neurons (**Fig. 1C**). Colocalization analysis showed that 20.7% (60 of 290) of *Atf4*-positive cells expressed *Mrgpra3* and 65.2% (202 of 310) of which expressed *H1R* (**Fig. 1C**). Researches have shown that TRP channels, particularly TRPA1 and TRPV1, play a significant role in the regulation of both acute and chronic pruritus.[25,44] The double immunostaining showed that ATF4 protein was expressed in TRPV1-positive and TRPA1-positive sensory neurons of mice (**Fig. 1D**). The proportion of ATF4-positive neurons expressing TRPV1 and TRPA1 was 45.8% (153 of 334) and 68.3% (192 of 281), respectively (**Fig. 1D**). Thus, the results demonstrate that ATF4 is expressed in most sensory neurons including those related to pruritus.

3.2. Loss of activated transcription factor 4 enhances the itch sensitivity of mice

To determine the role of ATF4 in pruritus, we intrathecally injected ATF4 siRNA to knockdown the expression of ATF4 in cervical DRGs (Supplementary Fig. 1b, c, http://links.lww.com/PAIN/C9). Behavioral results showed that knocking down of ATF4 led to an elevation in spontaneous scratching behaviors in mice (**Fig. 2A**). In both male and female mice, the number of scratch bouts increased in ATF4-siRNA-injected mice compared with nontargeting (NT)-siRNA injected mice following histamine treatment (**Figs. 2B and C** and Supplementary Fig. 1d, http://links.lww.com/PAIN/C9). Moreover, male and female mice injected with ATF4-siRNA exhibited enhancement in the number of scratch bouts when exposed to the nonhistaminergic pruritogen chloroquine (CQ, **Figs. 2D and E** and Supplementary Fig. 1e, http://links.lww.com/PAIN/C9). Sex did not affect the regulation of ATF4 on histamine- and CQ-induced pruritus (Supplementary Fig. 1d, e, http://links.lww.com/PAIN/C9). Furthermore, to investigate the specific role of ATF4 in pruritus regulation, we constructed *Atf4*-knockout mice. Considering that *Atf4* homozygous mice have postnatal lethality or functional defects,[41] we used heterozygous mice, both male and female, for the experiment. Activated transcription factor 4 protein expression in DRG neurons of *Atf4*$^{+/-}$ mice was lower than that of WT mice (**Figs. 1A and B**). Our previous work showed that *Atf4*$^{+/-}$ mice do not have developmental defects in sensory neurons and their innervations.[64] Behavioral results demonstrated that *Atf4*$^{+/-}$ mice exhibited increased spontaneous scratching behaviors compared with WT mice (**Fig. 2F**). In the disease state, harmless mechanical stimuli can cause pathological sensations,

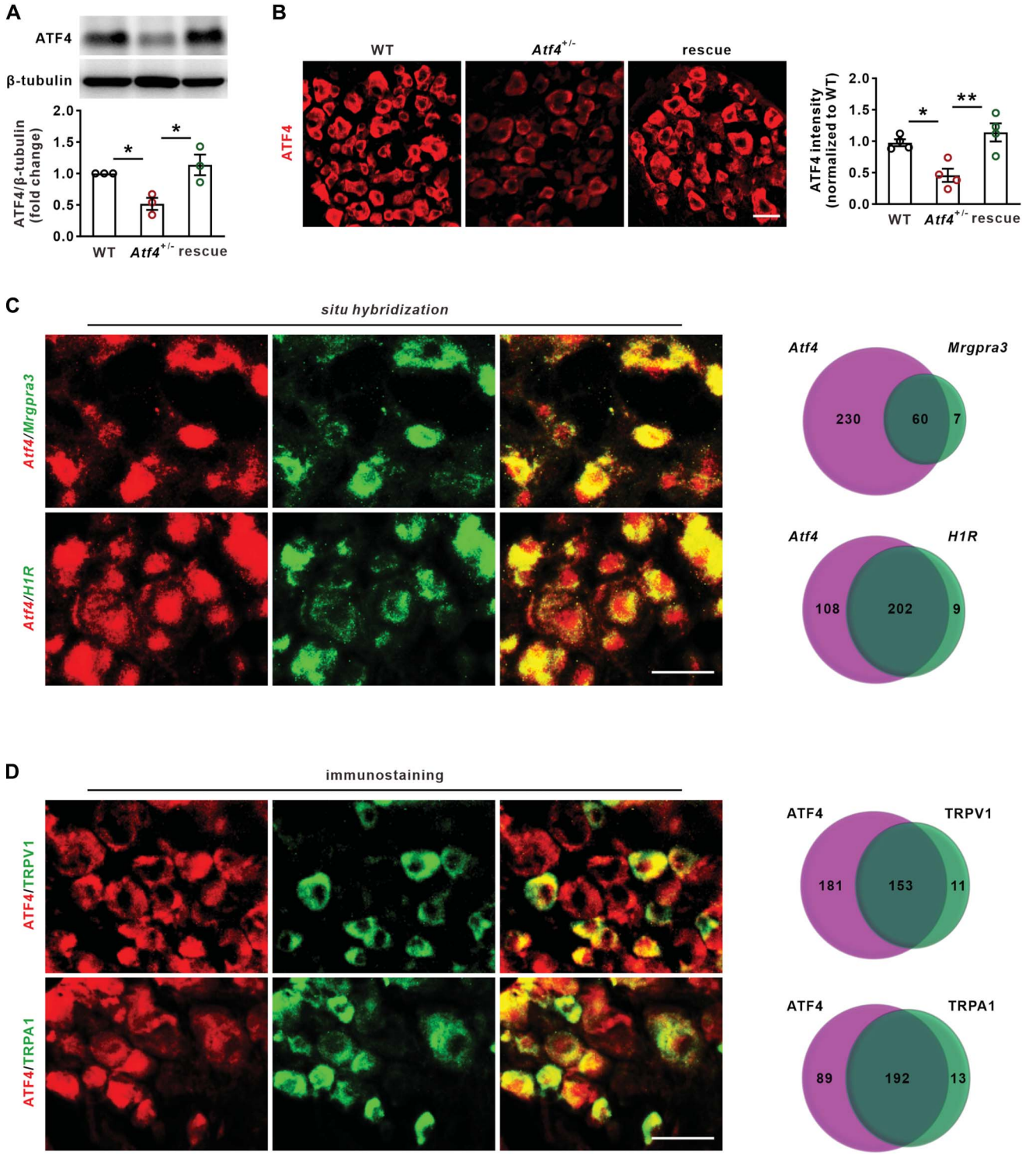

Figure 1. ATF4 is expressed in pruritus-related sensory neurons. (A) The expression of ATF4 was detected by immunoblotting in cervical DRGs of WT, *Atf4*$^{+/-}$, and rescue mice. n = 3 samples per group (2 mice mixed into a sample). (B) The expression of ATF4 was detected by immunohistochemistry in cervical DRGs of WT, *Atf4*$^{+/-}$, and rescue mice. n = 4 mice per group. Scale bar, 50 μm. (C) Double fluorescence in *situ hybridization* showed that the mRNA of *Atf4* was expressed in *Mrgpra3*$^{+}$ and *H1R*$^{+}$ cervical DRG neurons and Venn diagram showed the number of the overlap. Scale bar, 50 μm. (D) Colocalization of ATF4 protein with TRPV1 and TRPA1 in the cervical DRG sections and Venn diagram showed the number of the overlap. Scale bar, 50 μm. (A and B) One-way ANOVA followed by Tukey multiple comparisons test. *$P < 0.05$, **$P < 0.01$. The error bars indicate the SEMs. ANOVA, analysis of variance; ATF4, activated transcription factor 4; DRG, dorsal root ganglion; WT, wild-type.

such as mechanical pruritus.[19] Compared with WT mice, *Atf4*$^{+/-}$ mice displayed normal mechanically induced scratching to von Frey (Supplementary Fig. 2a, http://links.lww.com/PAIN/C9). The number of scratch bouts observed in *Atf4*$^{+/-}$ mice exhibited an increase compared with that in WT mice following both histamine (**Figs. 2G and H**) and CQ (**Figs. 2I and J**) treatments. To ascertain the role of ATF4 in chronic itch, it is worth noting that there are currently no effective treatments available.[43,56] Hence, we conducted tests on mice treated with diphenylcyclopropenone (DCP), a topical immunotherapy agent used for alopecia areata.

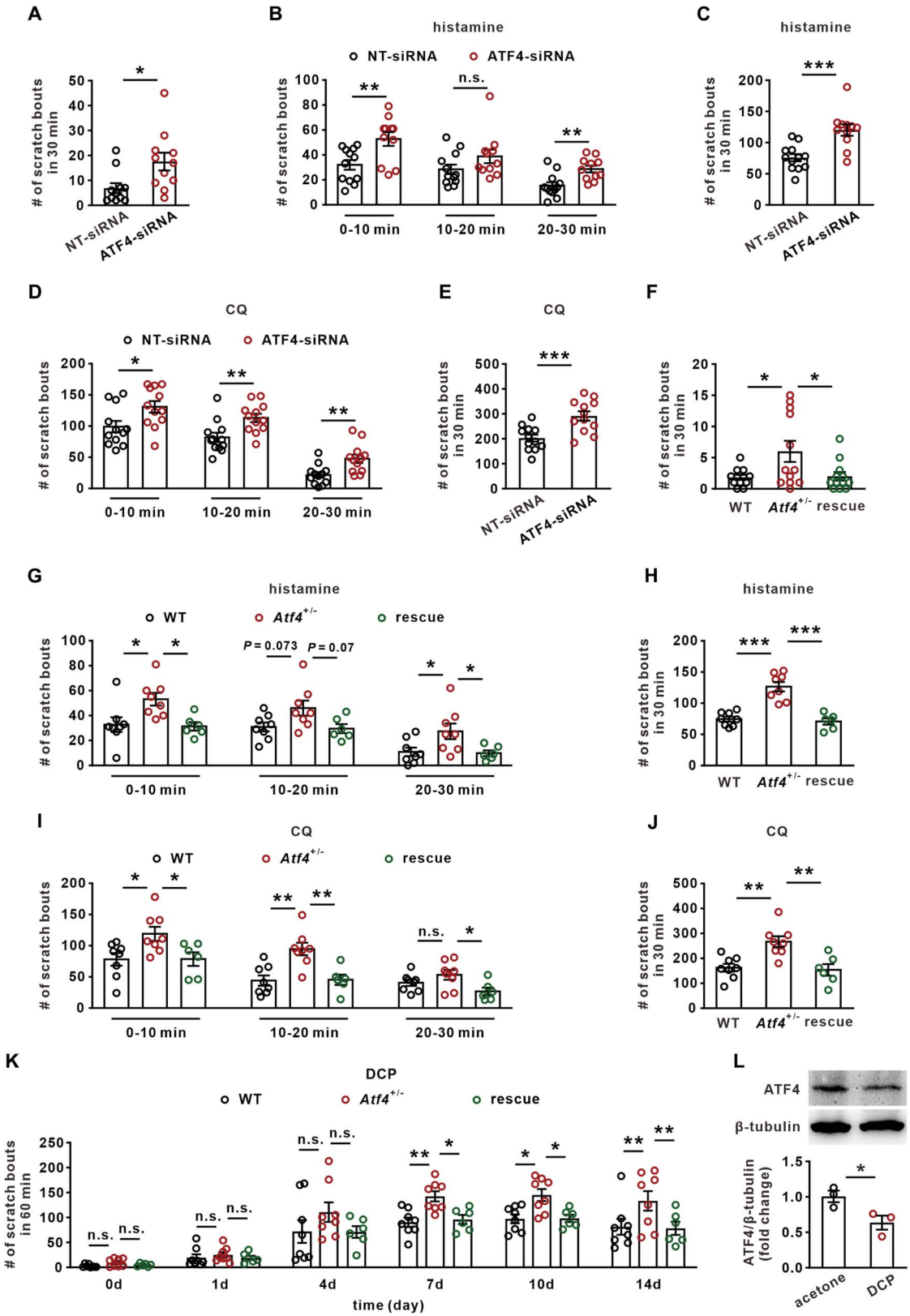

Figure 2. Loss of ATF4 intensifies the acute and chronic pruritus and rescue of ATF4 normalizes them. (A) The effect of intrathecal injecting ATF4-siRNA or NT-siRNA on the spontaneous scratching behaviors of mice. n = 11 mice per group. (B and C) The effect of intrathecal injection of ATF4-siRNA or NT-siRNA on the acute itch induced by histamine. n = 11-12 mice per group. (D and E) The effect of intrathecal injecting ATF4-siRNA or NT-siRNA on the acute itch induced by chloroquine (CQ). n = 12 mice per group. (F) The effect of deletion and reexpression of ATF4 on the spontaneous scratching behaviors. n = 12 mice per group. (G–J) The effect of deletion and re-expression of ATF4 on the acute itch induced by histamine and CQ. n = 6-8 mice per group. (K) The effect of deletion and re-expression of ATF4 on the chronic itch induced by diphenylcyclopropenone (DCP). n = 6-8 mice per group. (L) The effect of DCP treatment (day 14) on the ATF4 expression in cervical DRGs of WT mice. n = 3 samples per group (2 mice mixed into a sample). (A–E, L) Two-tailed independent Student *t* test; (F–J), One-way ANOVA followed by Tukey multiple comparisons test; (K), Two-way ANOVA followed by Bonferroni multiple comparisons test. $^{*}P < 0.05$, $^{**}P < 0.01$, $^{***}P < 0.001$, n.s, means not significant. The error bars indicate the SEMs. ANOVA, analysis of variance; ATF4, activated transcription factor 4; DRG, dorsal root ganglion; NT-siRNA, non-targeting siRNA; WT, wild-type.

However, it often leads to severe side effects, such as eczematous skin, contact dermatitis, and intense itching in both patients and mice.[55,58] WT mice treated with DCP showed increased and sustained scratching behavior, and deletion of ATF4 promoted the chronic itch behavior induced by DCP (**Fig. 2K**). Moreover, DCP treatment also significantly decreased the expression of ATF4 in cervical DRG tissues of WT mice (**Fig. 2L**). Thus, these results reveal that loss of ATF4 increases the itch sensitivity of mice.

3.3. Rescue of activated transcription factor 4 normalizes itch sensitivity in Atf4$^{+/-}$ mice

To further confirm the role of ATF4 in itch sensitivity, we intrathecally injected AAV delivery vector encoding ATF4 under the control of the neuronal promoter hSyn (rAAV-hSyn-*Atf4*-2A-EGFP) to rescue the expression of ATF4 in the cervical DRG neurons of *Atf4*$^{+/-}$ mice (rescued mice) and then subjected the rescued mice to behavioral tests. EGFP was observed in cervical DRG neurons of AAV-injected mice (Supplementary Fig. 2b, http://links.lww.com/PAIN/C9), confirming the transgene expression in the cervical DRG neurons. The expression of ATF4 was rescued in cervical DRG of *Atf4*$^{+/-}$ mice after intrathecally injected with rAAV-hSyn-*Atf4*-2A-EGFP (**Figs. 1A and B**). The behavioral data showed that rescuing of ATF4 can restore the spontaneous scratching behaviors in *Atf4*$^{+/-}$ mice to normal levels (**Fig. 2F**). Activated transcription factor 4 rescued mice displayed normal mechanically induced scratching to von Frey (Supplementary Fig. 2a, http://links.lww.com/PAIN/C9). Compared with *Atf4*$^{+/-}$ mice, the number of scratch bouts was decreased in rescued mice following histamine and CQ treatments (**Figs. 2G–J**). The restoration of ATF4 clearly counteracted the promoting effect caused by ATF4 deletion on the chronic itching induced by DCP (**Fig. 2K**). Thus, these data indicate that rescue of ATF4 normalizes the itch sensitivity in *Atf4*$^{+/-}$ mice, suggesting that ATF4 is necessary for the itch signal transduction.

3.4. Overexpression of activated transcription factor 4 alleviates the acute and chronic pruritus

Furthermore, we intrathecally injected AAV delivery vector encoding ATF4 (rAAV-hSyn-*Atf4*-2A-EGFP) in WT mice to overexpress ATF4 in the cervical DRG neurons (Supplementary Fig. 3a, b, http://links.lww.com/PAIN/C9). There was no difference in spontaneous scratching behaviors between the ATF4 overexpression and control mice (**Fig. 3A**). Overexpression of ATF4 significantly remitted histamine-, CQ-, and SLIGRL-induced (PAR-2 agonist) acute pruritus (**Figs. 3B–F**). In comparison to the control group, ATF4 overexpression mitigated the chronic itching behavior induced by DCP and DNFB (allergic contact dermatitis model) in mice (**Figs. 3G and H**). Because ATF4 is also expressed in the brain[48] and spinal cord,[64] we next determined the specific role of ATF4 in DRG neurons. To achieve this, we locally injected AAV encoding ATF4 (rAAV-hSyn-*Atf4*-2A-EGFP) into the spinal nerves just distal to the DRGs at the cervical segments (C3 and C4). In mice injected with AAV solution, EGFP was observed in DRG neurons (Supplementary Fig. 4a, http://links.lww.com/PAIN/C9), confirming the transgene expression in the cervical DRG neurons. The expression of ATF4 was also increased in cervical DRG after local injection with rAAV-hSyn-*Atf4*-2A-EGFP (Supplementary Fig. 4b, c, http://links.lww.com/PAIN/C9). Behavioral data showed that local cervical DRG overexpression of ATF4 did not alter spontaneous scratching behaviors in mice (**Fig. 3I**) but significantly reduced acute pruritus behavior induced by histamine and CQ (**Figs. 3J–M**). Compared with the control group, local injection of AAV encoding ATF4 to overexpress ATF4 in cervical DRG significantly alleviated chronic itch induced by DCP (**Fig. 3N**). These results suggest that ATF4 expression in primary afferent sensory neurons is critical in regulating acute and chronic itch behavior.

3.5. Loss of activated transcription factor 4 increases the activity of sensory neurons induced by pruritogen

Subsequently, we employed in vivo intracellular calcium imaging as a method to measure the activity of primary sensory neurons, to investigate whether ATF4 had an impact on neuronal activity. *Atf4*$^{+/-}$ and WT mice were injected intrathecally with AAV delivery vector encoding the calcium indicator GCaMP6 (rAAV-CAG-*GCaMp6s*). The change of fluorescence signal after the application of pruritogen in the hind paw indicates the activity of DRG neurons (**Fig. 4A**). Following injection of either histamine (2 μg/μL, 5 μL) or CQ (4 μg/μL, 5 μL) into the ipsilateral hindpaw, we observed robust activation of sensory neurons in L4 DRG (**Figs. 4A–E**). Histamine and CQ activated a comparable proportion of sensory neurons in WT mice (**Figs. 4B and D**), whereas both pruritogens activated a higher percentage of neurons in *Atf4*$^{+/-}$ mice (**Figs. 4B and D**). Furthermore, we isolated the neuronal response by cell profile area and found that histamine and CQ primarily elevated the activation of small-sized (<500 μm^2) and medium-sized (500-1000 μm^2) DRG neurons in *Atf4*$^{+/-}$ mice (**Figs. 4C and E**). Consistently, both small-sized (<500 μm^2) and medium-sized (500-1000 μm^2) DRG neurons from *Atf4*$^{+/-}$mice exhibited larger increases in intracellular calcium following pruritogen stimulation (**Figs. 4F and G**). In comparison to WT mice, the medium-sized DRG neurons exhibited a pronounced hyperresponsiveness to histamine (**Fig. 4F**) and CQ (**Fig. 4G**) stimulation applied to the hindpaw in *Atf4*$^{+/-}$mice. However, small-sized DRG neurons from *Atf4*$^{+/-}$ mice were also more responsive to histamine application (**Fig. 4F**). In addition, we detected the individual neuron responses in the 30 minutes period after histamine injection. We observed that the neuronal responses were distributed throughout the entire recording period, rather than being concentrated solely in the early stages of histamine injection (**Fig. 4H**), which is consistent with the duration of scratch responses. Therefore, these findings suggest that ATF4 is involved in the regulation of sensory neuron activity following pruritogen stimulation.

3.6. Activated transcription factor 4 interacts with transient receptor potential cation channel subfamily V member 4 in sensory neurons

Histamine-induced itch typically involves histamine receptor type 1 (H1R) and/or type 4 (H4R),[7,26] whereas CQ-induced itch stimulates MrgprA3.[37] To further elucidate the potential mechanisms by which ATF4 regulates itching, we initially investigated whether ATF4 has a regulatory role in the expression of H1R, H4R, and MrgprA3. The results showed that, in comparison to WT mice, the mRNA expression levels of *H1R*, *H4R*, and *MrgprA3* in *Atf4*$^{+/-}$ mouse DRG did not show significant changes (Supplementary Fig. 5a-c, http://links.lww.com/PAIN/C9). This indicates that ATF4 is not involved in regulating the expression of H1R, H4R, or MrgprA3. Although more than a dozen TRPs have been identified in DRG neurons,[59] to date, only TRPV1, TRPA1, and TRPV4 channels have been implicated in itch signaling in sensory neurons.[6,44] Our research and that of our peers have shown that ATF4 can directly interact with ion channels or receptors in

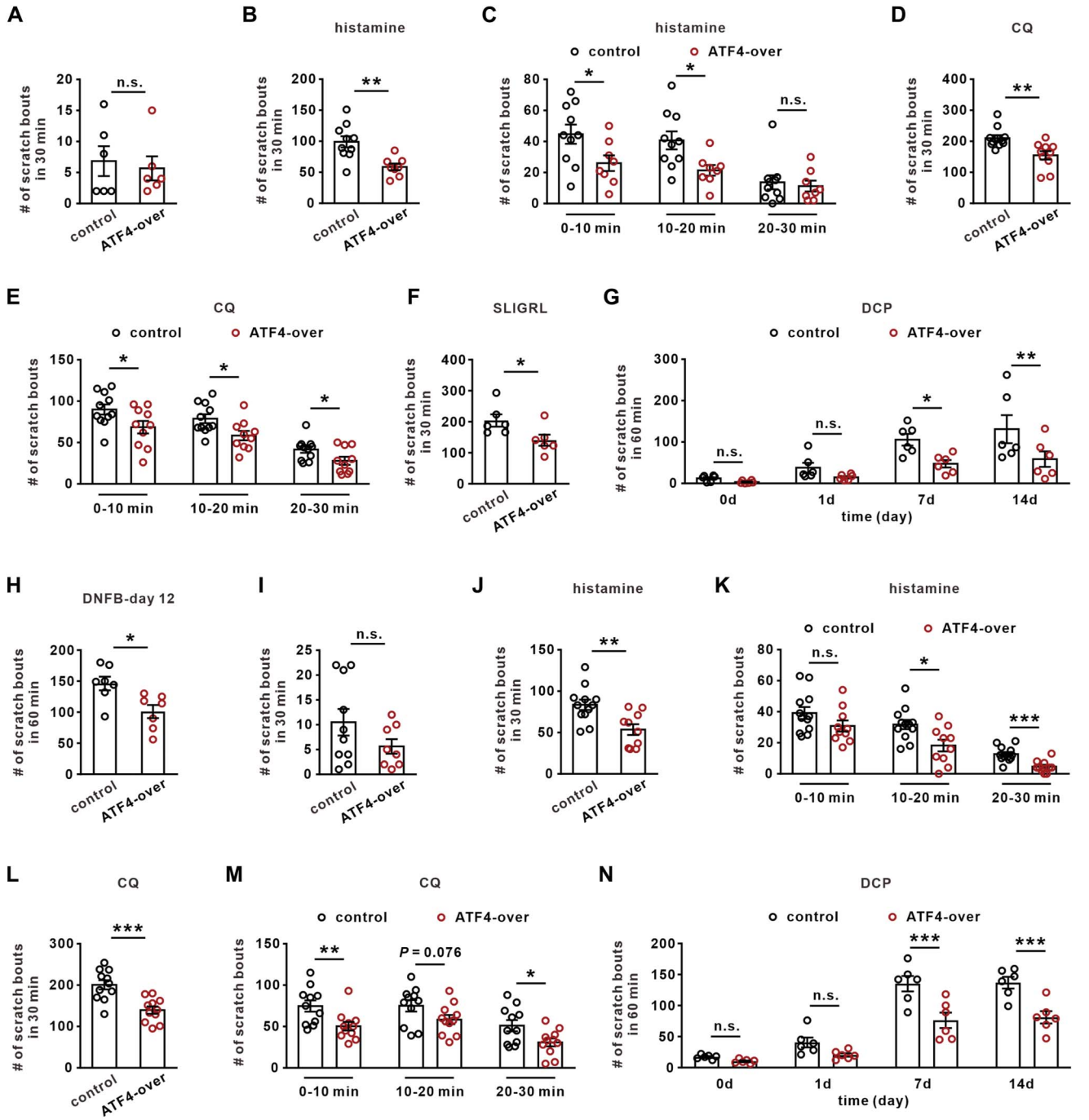

Figure 3. Overexpression of ATF4 alleviates the acute and chronic pruritus. (A) The effect of intrathecal injection of AAV-expressing ATF4 (rAAV-hSyn-*Atf4*-2A-EGFP) on the spontaneous scratching behaviors of mice. n = 6 mice per group. (B–F) The effect of intrathecal injection of AAV-expressing ATF4 (rAAV-hSyn-*Atf4*-2A-EGFP) on the acute itch induced by histamine, CQ, and Ser-Leu-Ile-Gly-Arg-Leu-NH2 (SLIGRL, PAR-2 agonist). n = 6-11 mice per group. (G, H) The effect of intrathecal injection of AAV-expressing ATF4 (rAAV-hSyn-*Atf4*-2A-EGFP) on the chronic itch induced by DCP and 1-fluoro-2, 4-dinitrobenzene (DNFB). n = 6-7 mice per group. (I) The effect of spinal nerve injection of AAV-expressing ATF4 (rAAV-hSyn-*Atf4*-2A-EGFP) on the spontaneous scratching behaviors of mice. n = 8-10 mice per group. (J–M) The effect of spinal nerve injection of AAV-expressing ATF4 (rAAV-hSyn-*Atf4*-2A-EGFP) on the acute itch induced by histamine and CQ. n = 10-12 mice per group. (N) The effect of spinal nerve injection of AAV-expressing ATF4 (rAAV-hSyn-*Atf4*-2A-EGFP) on the chronic itch induced by DCP. n = 6 mice per group. (A–F, H–M) Two-tailed independent Student *t* test; (G, N), 2-way ANOVA followed by Bonferroni multiple comparisons test. $^{*}P < 0.05$, $^{**}P < 0.01$, $^{***}P < 0.001$, n.s, means not significant. The error bars indicate the SEMs. AAV, adenoassociated virus; CQ, chloroquine; DCP, diphenylcyclopropenone; EGFP, enhanced green fluorescent protein.

neurons.45,50,60,64 Furthermore, we investigated whether ATF4 interacts with TRPV1, TRPA1, and TRPV4 channels in DRG neurons. The Co-IP data revealed a potential interaction of ATF4 with TRPV4 channels (**Fig. 5A**) and almost no interaction with TRPA1 or TRPV1 channels (**Figs. 5B and C**) in mouse DRG protein extracts. Double staining showed that ATF4 colocalized with TRPV4 in mouse DRG neurons (**Fig. 5D**). In addition, we performed high-resolution imaging by structured illumination microscopy (SIM) and found that ATF4 colocalized with TRPV4 in sensory neurons (**Fig. 5E**). To further confirm the possible ATF4/TRPV4 interaction, we used the PLA in isolated DRG neurons.[61] Proximity ligation assay analysis revealed positive fluorescence signals on

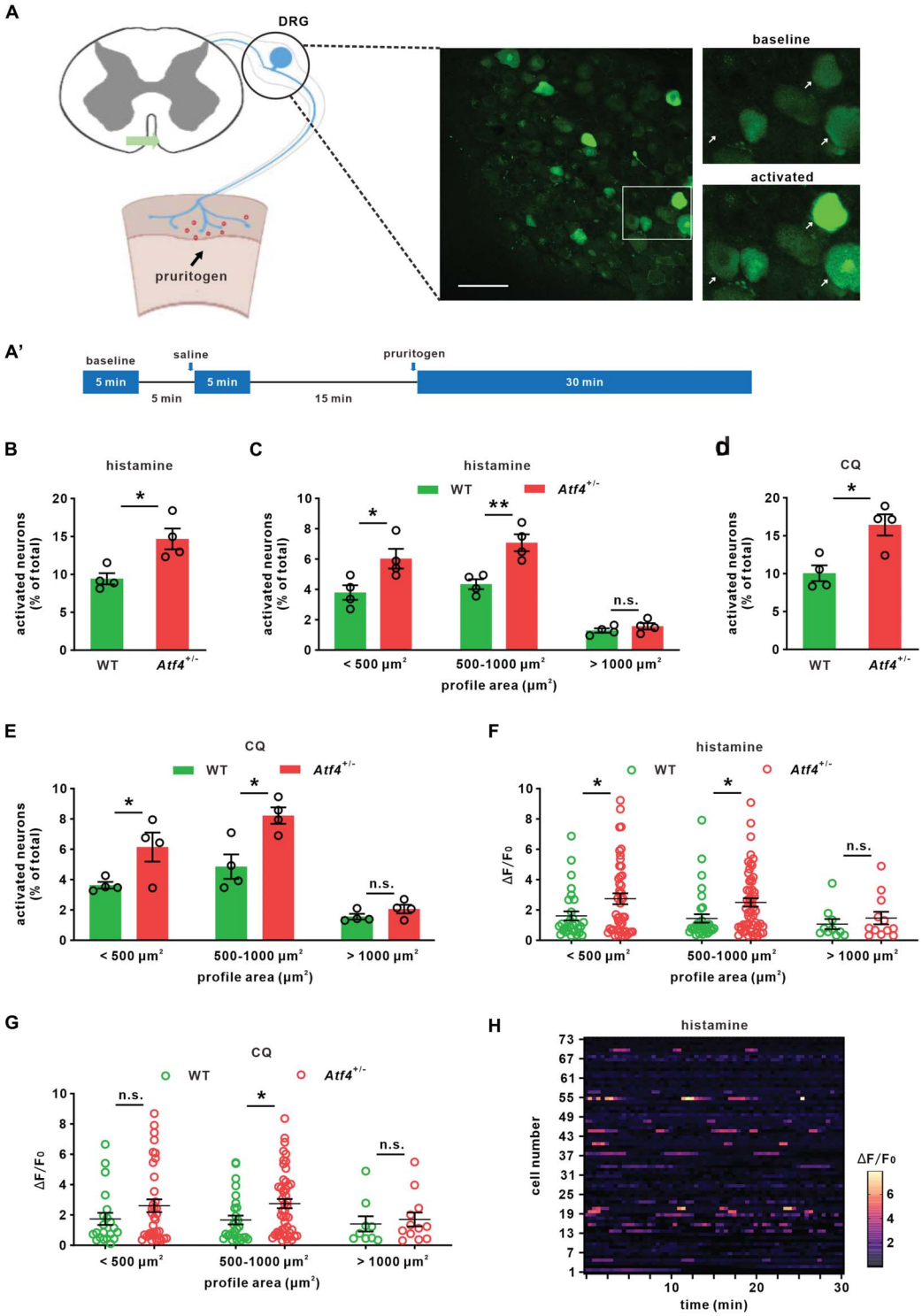

Figure 4. In vivo calcium imaging shows that DRG neurons from *Atf4*$^{+/-}$ mice are hyperresponsive to pruritogen stimuli. (A and A') Schematic diagram for the in vivo calcium imaging of sensory neurons and the representative images of GCaMP6 fluorescence as a measure of intracellular calcium following pruritogen stimulation to the hindpaw. White arrows indicate activated neurons. Scale bar, 100 μm. (B) The total rate of activated DRG neurons after hindpaw injection of histamine in WT and *Atf4*$^{+/-}$ mice. Empty circles represent imaging trials from independent mice. n = 4 mice per group. (C) The diameter distribution of the proportion of activated DRG neurons after hindpaw injection of histamine in WT and *Atf4*$^{+/-}$ mice. Empty circles represent imaging trials from independent mice. n = 4 mice per group. (D and E) The overall and diameter distribution of the proportion of activated DRG neurons induced by CQ in WT and *Atf4*$^{+/-}$ mice. Empty circles represent imaging trials from independent mice. n = 4 mice per group. (F) In comparison to control, small-sized and medium-sized DRG neurons in *Atf4*$^{+/-}$ mice showed significantly increased responses to histamine stimulation (<500 μm^2 WT, n = 29 cells; *Atf4*$^{+/-}$, n = 46 cells; 500-1000 μm^2 WT, n = 34 cells; *Atf4*$^{+/-}$, n = 54 cells). (G) Compared with WT mice, DRG neurons from *Atf4*$^{+/-}$ mice also had a significantly greater response to CQ stimulation applied to the glabrous skin. This was particularly true of medium-sized cells (500-1000 μm^2 WT, n = 28 cells; *Atf4*$^{+/-}$, n = 48 cells). (H) The heatmaps of individual neurons activated by histamine in WT mice (n = 73 cells). (B–G) Two-tailed independent Student *t* test. *$P < 0.05$, **$P < 0.01$, n.s, means not significant. The error bars indicate the SEMs. CQ, chloroquine; DRG, dorsal root ganglion; WT, wild-type.

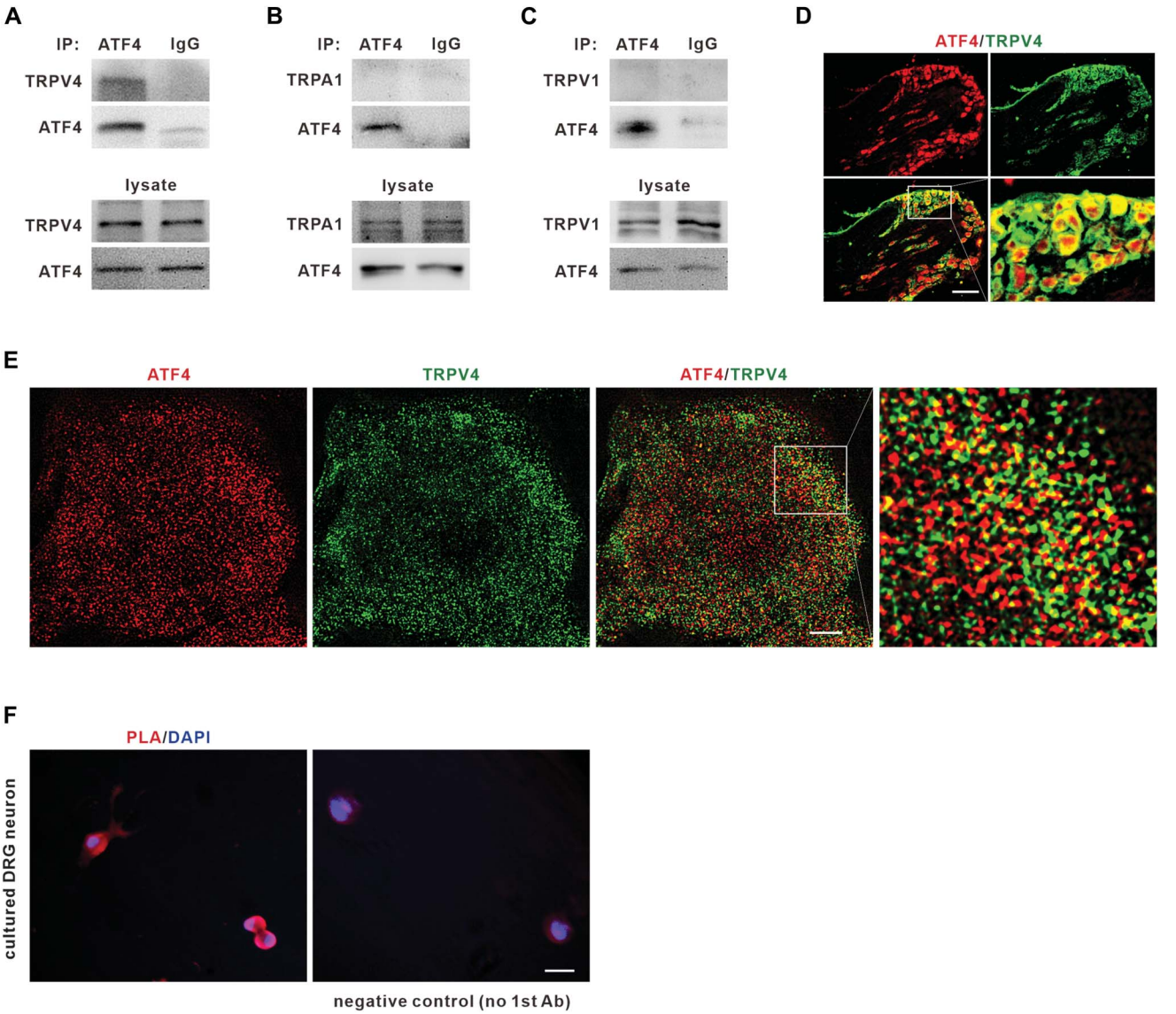

Figure 5. ATF4 interacts with TRPV4 in sensory neurons. (A–C) Co-IP results showed that ATF4 interacted with TRPV4 in DRGs. DRG lysates were immunoprecipitated with ATF4 antibody and immunoblotted with TRPV4, TRPA1, TRPV1, and ATF4 antibody as indicated. This experiment was repeated 3 times. (D) Double immunostaining of ATF4 and TRPV4 in cervical DRG sections. Scale bar, 200 μm. (E) The high-resolution images show that the colocalization between ATF4 and TRPV4 in cervical DRG neurons of mice. Scale bar, 5 μm. (F) Proximity ligation assay (PLA) showed positive signals of ATF4/TRPV4 interaction in cultured DRG neurons, and staining was absent in negative control with omission of primary antibody (6 images from 2 repeats). Scale bar, 20 μm. ATF4, activated transcription factor 4; DRG, dorsal root ganglion; TRPV4, transient receptor potential cation channel subfamily V member 4.

cell bodies in cultured mouse DRG neurons, and staining was absent in negative control group (**Fig. 5F**). These results indicate close proximity of ATF4 and TRPV4 and possible interaction between these 2 molecules in sensory neurons.

3.7. Activated transcription factor 4 inhibits the function of transient receptor potential cation channel subfamily V member 4 in sensory neurons

Furthermore, we investigated the role of ATF4 in regulating the membrane, cytoplasm, and total expression of TRPV4 in DRGs. The data showed that knockdown of ATF4 did not change the membrane (Supplementary Fig. 6a, http://links.lww.com/PAIN/C9), cytoplasm (Supplementary Fig. 6b, http://links.lww.com/PAIN/C9), or total (Supplementary Fig. 6c, http://links.lww.com/PAIN/C9) expression of TRPV4 in DRGs of mice. Compared with WT mice, the expression of TRPV4 in membrane, cytoplasm, and total were comparable in DRGs of *Atf4*$^{+/-}$ mice (Supplementary Fig. 6d-f, http://links.lww.com/PAIN/C9). Surface biotinylation analysis revealed that the deletion of ATF4 did not affect the membrane trafficking of TRPV4 in DRG neurons (Supplementary Fig. 6g, http://links.lww.com/PAIN/C9). Consistently, overexpression of ATF4 did not alter the membrane (Supplementary Fig. 6h, http://links.lww.com/PAIN/C9), cytoplasm (Supplementary Fig. 6i, http://links.lww.com/PAIN/C9), or total (Supplementary Fig. 6j, http://links.lww.com/PAIN/C9) abundance of TRPV4 in DRGs of mice. Thus, interference with ATF4 does not alter the expression and trafficking of TRPV4 in sensory neurons. Considering that ATF4 does not affect the expression and membrane trafficking of TRPV4 and that ATF4 interacts with TRPV4 in DRG neurons, we speculated that ATF4 may regulate the function of TRPV4 channels. To further confirm whether ATF4 regulated the function of TRPV4, whole-cell patch clamp experiments were performed in DRG neurons. Compared with WT mice, 4-αPDD–induced (TRPV4 agonist, 10 μM)[22] currents were increased in DRG neurons of *Atf4*$^{+/-}$ mice (**Figs. 6A and B**).

Importantly, rescue of ATF4 in *Atf4*$^{+/-}$ mice significantly reduced the 4-αPDD–induced currents in DRG neurons (**Figs. 6A and B**). Furthermore, we examined another TRPV4 agonist–induced (GSK101, 1 μM)[33] Ca^{2+} responses in dissociated DRG neurons using vitro calcium imaging. The data showed that compared with WT mice, GSK101 induced an increased Ca^{2+} responses in DRG neurons of *Atf4*$^{+/-}$ mice and reexpression of ATF4 normalized the Ca^{2+} response (**Figs. 6C–E**). To further determine whether ATF4 also modulates the TRPV1 and TRPA1 channels, we examined the Ca^{2+} responses to capsaicin[21] (TRPV1 agonist) and AITC[2] (TRPA1 agonist) treatments in WT and *Atf4*$^{+/-}$ DRG neurons. The results showed that capsaicin-induced Ca^{2+} responses in DRG neurons were comparable between WT and *Atf4*$^{+/-}$ mice (Supplementary Fig. 7a, http://links.lww.com/PAIN/C9). In comparison to WT mice, the Ca^{2+} responses in DRG neurons induced by AITC were not observed to be altered in *Atf4*$^{+/-}$ mice (Supplementary Fig. 7b, http://links.lww.com/PAIN/C9). This indicates that ATF4 is not involved in regulating the function of TRPV1 and TRPA1 channels in sensory neurons. Furthermore, we investigated the regulatory effect of overexpressing ATF4 on TRPV4 current in sensory neurons. Compared with the control group, overexpression of ATF4 significantly decreased the TRPV4 currents induced by 4-αPDD in sensory neurons (**Figs. 6F and G**). Therefore, this suggests that ATF4 inhibits the function of TRPV4 in sensory neurons. To further examine whether ATF4 regulates itching through the TRPV4 channel, we intraperitoneally administered a specific TRPV4 antagonist HC 067,047 (HC; 10 mg/kg)[18,33] to WT and *Atf4*$^{+/-}$ mice and subsequently observed its effects on acute and chronic itching. The results showed that when compared with the *Atf4*$^{+/-}$ + vehicle group, the *Atf4*$^{+/-}$ + HC group displayed a significant reduction in acute scratch bouts induced by histamine and CQ (**Figs. 6H and I**). Blocking the TRPV4 channel also suppressed the augmented effect of ATF4 deficiency on chronic itching induced by DCP (**Fig. 6J**). Therefore, these results suggest that ATF4 exerts its regulatory role on itching through the TRPV4 channel. Activated transcription factor 4 is known to regulate gene transcription through its basic leucine zipper (bZIP) domain.[23] To further exclude the effect of the transcriptional function of ATF4, a transcription factor, on TRPV4 channels, we overexpressed a transcriptionally inactive form of ATF4 (mutation of bZIP: ΔbZIP) in DRG of WT mice by intrathecal injected rAAV-hSyn-*Atf4*-ΔbZIP. The transcriptionally inactive form of ATF4 was generated by site-directed mutagenesis with 7 amino acid substitutions within the DNA-binding domain (^{292}RYRQKKR^{298} to ^{292}GYLEAAA^{298}).16,27,53 The data showed that overexpression of a transcriptionally inactive form of ATF4 also did not alter the membrane, cytoplasm, or total expression of TRPV4 in sensory neurons (**Figs. 7A–C**). Notably, compared with the control group, overexpression of a transcriptionally inactive form of ATF4 significantly decreased the TRPV4 currents induced by 4-αPDD in sensory neurons (**Figs. 7D and E**). Consistently, overexpression of a transcriptionally inactive form of ATF4 significantly alleviated histamine-induced and CQ-induced acute pruritus and also reduced DCP-induced chronic pruritus in mice (**Figs. 7F–H**). Thus, ATF4 interacts with TRPV4 and exerts a significant inhibitory effect on its function in a nontranscriptional manner in DRG neurons.

3.8. Activated transcription factor 4 regulates the function of TRPV4 through 117-232 aa fragments

To determine how ATF4 interacted with TRPV4, we constructed 3 expression vectors, namely, ATF4-His (1-116 aa), ATF4-His (117-232 aa), and ATF4-His (233-349 aa), and coexpressed them with the TRPV4-Flag in HEK293T cells. Co-IP analysis showed that the 117-232 aa region of ATF4 was found to be the major binding site for TRPV4 (**Fig. 8A**). To further investigate the function of ATF4 117-232 aa region, we intrathecally injected rAAV-hSyn-*Atf4-His (117-232)*-2A-EGFP to overexpress 117-232 aa region in DRG neurons of WT mice (**Fig. 8B**). The behavioral data indicated that there was no significant difference in spontaneous scratching behaviors between the mice with overexpression of the 117-232 aa region and the control group (**Fig. 8C**). Overexpression of the 117-232 aa region significantly reduced histamine-evoked and CQ-evoked acute pruritus (**Figs. 8D and E**). Compared with the control group, overexpression of the 117-232 aa region also lessened DCP-evoked scratching behavior in mice (**Fig. 8F**). Moreover, compared with the control group, overexpression of the 117-232 aa region markedly reduced the current of TRPV4 evoked by 4-αPDD in sensory neurons (**Figs. 8G and H**). Furthermore, we intrathecally injected rAAV-hSyn-*Atf4-His (117-232)*-2A-EGFP in *Atf4*$^{+/-}$ mice to confirm the function of the 117-232 aa region. The data showed that intrathecal injection of rAAV-hSyn-*Atf4-His (117-232)*-2A-EGFP significantly decreased the number of scratch bouts induced by histamine, CQ, and DCP in *Atf4*$^{+/-}$ mice (**Figs. 8I–K**). Therefore, these results indicate that ATF4 may regulate itch sensation behavior and the function of TRPV4 through its 117-232 aa fragments.

3.9. Interference with activated transcription factor 4 increases itch sensitivity in nonhuman primates, and activated transcription factor 4 colocalizes with transient receptor potential cation channel subfamily V member 4 in human sensory neurons

Nonhuman primates have been tested for sensory research because of their phylogenetic proximity to humans.[15] Double immunostaining showed that ATF4 colocalized with TRPV4 in monkey DRG neurons (**Fig. 9A**). Furthermore, we tested whether intrathecal injection of ATF4-siRNA affected the itch sensitivity in nonhuman primates (**Fig. 9B**). The knockdown effect of ATF4-siRNA was verified in monkey vero cells (**Fig. 9C**). The behavioral data showed that ATF4-siRNA increased the spontaneous scratching behaviors in nonhuman primates (**Fig. 9D**). We then plantar injected histamine to establish the acute itch model in nonhuman primates. Notably, ATF4-siRNA also increased the number of scratch bouts induced by histamine in nonhuman primates (**Fig. 9E**). Moreover, ATF4-siRNA markedly increased the TRPV4 currents induced by 4-αPDD in sensory neurons of nonhuman primates (**Figs. 9F and G**). Therefore, these results suggest that in nonhuman primates, ATF4 may also be involved in regulating itch sensitivity by modulating the function of TRPV4. To evaluate the translational potential of this study, we further tested the distribution pattern of ATF4 in human DRG sections. Immunostaining showed that ATF4 was colocalized with TRPV4 in human DRG neurons (**Fig. 9H**). High-resolution images confirmed the colocalization of ATF4 and TRPV4 in human DRG neurons (**Fig. 9I**), and also indicated that the 2 proteins were close together. Therefore, ATF4 is involved in the regulation of itch sensitivity in nonhuman primates, and ATF4 colocalizes with TRPV4 in human sensory neurons.

4. Discussion

In this study, we have revealed that ATF4 is distributed in pruritus-related sensory neurons and interacts with TRPV4 to inhibit the

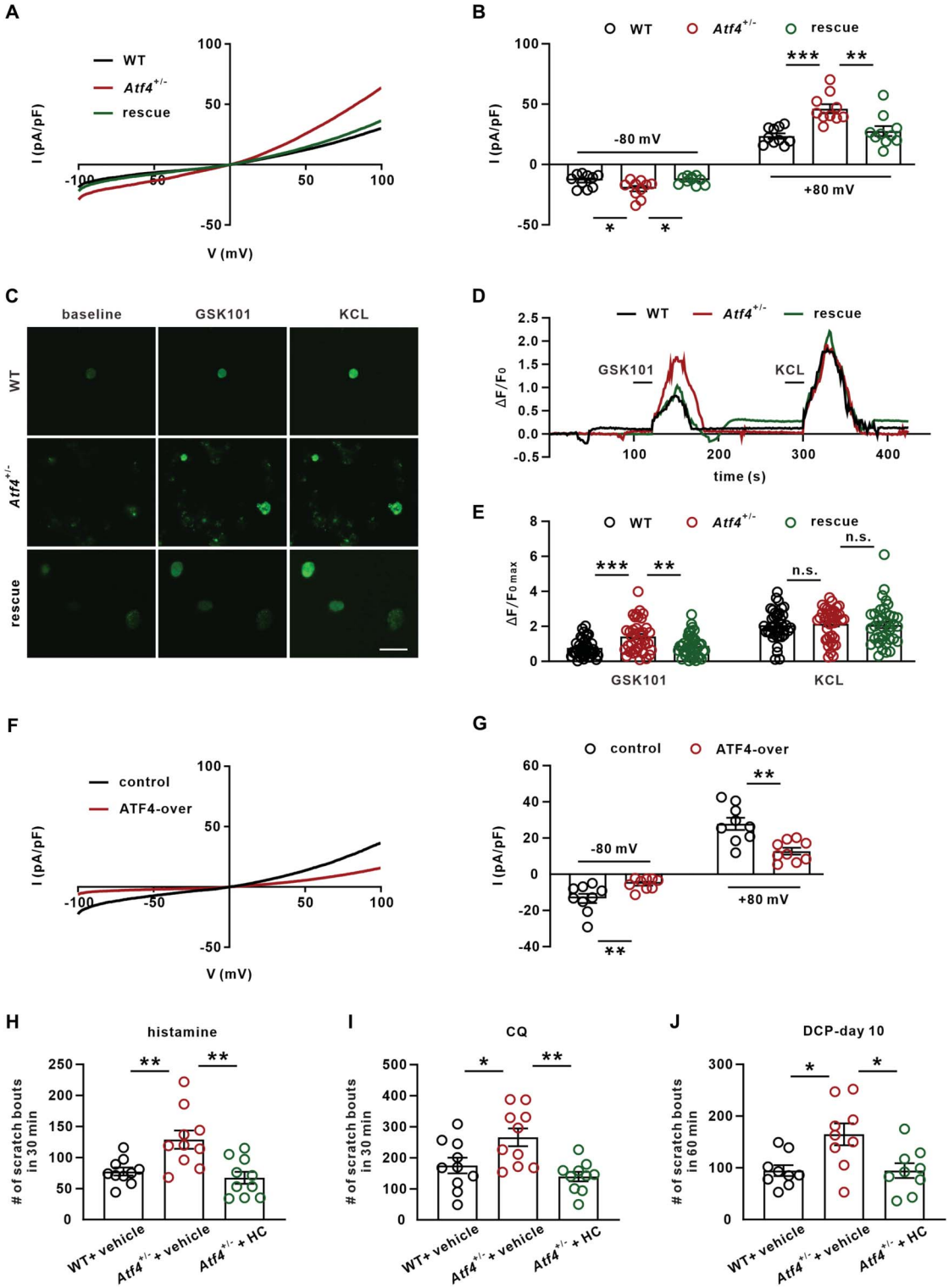

Figure 6. ATF4 inhibits the function of TRPV4. (A and B) The effect of deletion and reexpression of ATF4 on the current density of TRPV4 induced by 4-αPDD (TRPV4 agonist, 10 μM) in sensory neurons. n = 10 neurons per group. (C) Representative images of calcium responses to GSK101 (TRPV4 agonist, 1 μM) and KCL (40 mM) sequentially in sensory neurons from WT, *Atf4*$^{+/-}$, and rescued mice. Scale bar, 50 μm. (D) Representative traces show a neuronal calcium response to GSK101 (TRPV4 agonist, 1 μM) and KCL (40 mM) in sensory neurons from WT, *Atf4*$^{+/-}$, and rescued mice. (E) The effect of deletion and reexpression of ATF4 on the maximum Ca^{2+} responses induced by GSK101 (TRPV4 agonist, 1 μM) and KCL (40 mM) in sensory neurons. n = 38 to 40 neurons per group. (F and G) The effect of overexpression of ATF4 on the current density of TRPV4 induced by 4-αPDD (TRPV4 agonist, 10 μM) in sensory neurons. n = 9 neurons per group. (H–J) Scratching responses in WT and *Atf4*$^{+/-}$ mice preinjected (intraperitoneal) with vehicle control or TRPV4 antagonist HC (10 mg/kg) followed by histamine, CQ, or DCP. n = 9 to 10 mice per group. (B, E, H–J) One-way ANOVA followed by Tukey multiple comparisons test; (G), 2-tailed independent Student *t* test. *$P < 0.05$, **$P < 0.01$, ***$P < 0.001$, n.s, means not significant. The error bars indicate the SEMs. ANOVA, analysis of variance; ATF4, activated transcription factor 4; CQ, chloroquine; DCP, diphenylcyclopropenone; TRPV4, transient receptor potential cation channel subfamily V member 4; WT, wild-type; HC, 2-Methyl-1-[3-(4-morpholinyl)propyl]-5-phenyl-N-[3-(trifluoromethyl)phenyl]-1H-pyrrole-3-carboxamide HC067074; 4-αPDD, 4α-Phorbol-12,13-didecanoate.

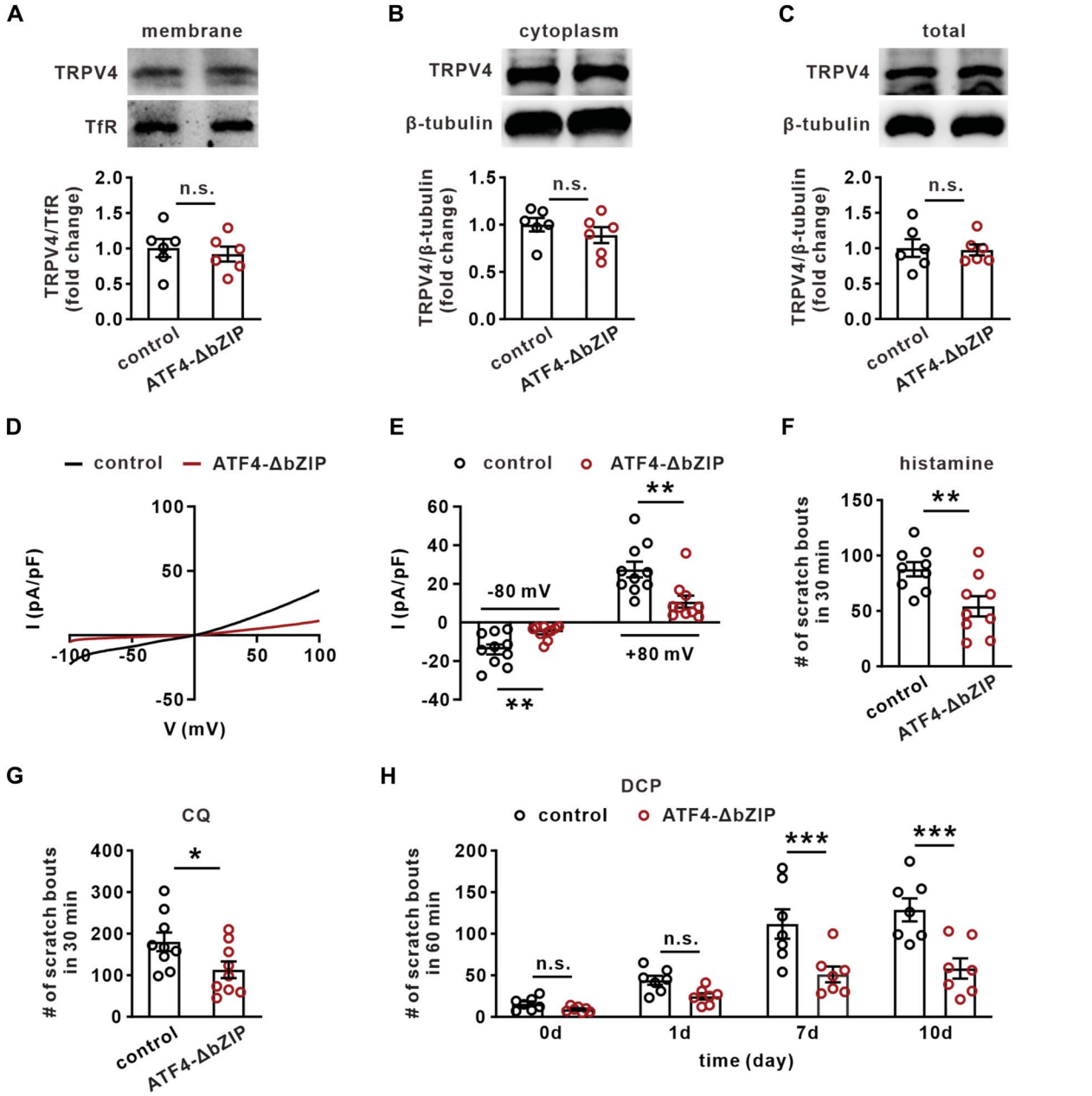

Figure 7. Overexpressing a transcriptionally inactive form of ATF4 alleviates the acute, chronic pruritus and reduces the current of TRPV4. (A–C) The effect of overexpressing a transcriptionally inactive form of ATF4 on the membrane (A), cytoplasm (B), and total (C) expression of TRPV4 in DRGs. n = 6 samples per group (2 mice mixed into a sample). (D and E) The effect of overexpressing a transcriptionally inactive form of ATF4 on the TRPV4 current induced by 4-αPDD (TRPV4 agonist, 10 μM) in sensory neurons. n = 10 neurons per group. (F and G) The effect of overexpressing a transcriptionally inactive form of ATF4 on the acute itch induced by histamine and CQ. n = 9 mice per group. (H) The effect of overexpressing a transcriptionally inactive form of ATF4 on the chronic itch induced by DCP. n = 7 mice per group. (A–C, E–G) Two-tailed independent Student *t* test; (H), 2-way ANOVA followed by Bonferroni multiple comparisons test. $^{*}P < 0.05$, $^{**}P < 0.01$, $^{***}P < 0.001$, n.s, means not significant. The error bars indicate the SEMs. ANOVA, analysis of variance; ATF4, activated transcription factor 4; CQ, chloroquine; DCP, diphenylcyclopropenone; DRG, dorsal root ganglion; TRPV4, transient receptor potential cation channel subfamily V member 4; 4-αPDD, 4α-Phorbol-12,13-didecanoate.

function of TRPV4 in sensory neurons in a nontranscriptional form, thereby regulating itch perception (**Fig. 10**). Activated transcription factor 4, also known as cAMP response element-binding protein 2 (CREB-2), is a member of the ATF/CREB transcription factor family, mainly involved in gene transcriptional regulation.[32] ATF4 is widely expressed in various tissues, playing a crucial role in regulating diverse physiological and pathological processes. Specifically, it is integral to the development of skeletal and lens tissues; the absence of ATF4 has been linked to hypoplasia in these structures.[17,57] In the hippocampal neurons, ATF4 participates in the regulation of synaptic plasticity and memory formation.[8,12] In the cerebral cortex of Alzheimer disease (AD), the level of ATF4 protein increases to 1.9 times that of controls.[47] In addition, locally synthesized ATF4 in axons is proposed to act as a mediator for the spread of the neurodegenerative signal in AD pathology.[3] This suggests its potential role as a downstream signal of Aβ. Previous studies by us and our peers have shown that ATF4 is abundantly expressed in primary sensory neurons and is involved in the regulation of joint traction pain and thermal nociception.[14,64] Our data show that ATF4 is expressed in pruritus-related sensory neurons in mice. Knocking down of ATF4 in DRG neurons increased the spontaneous

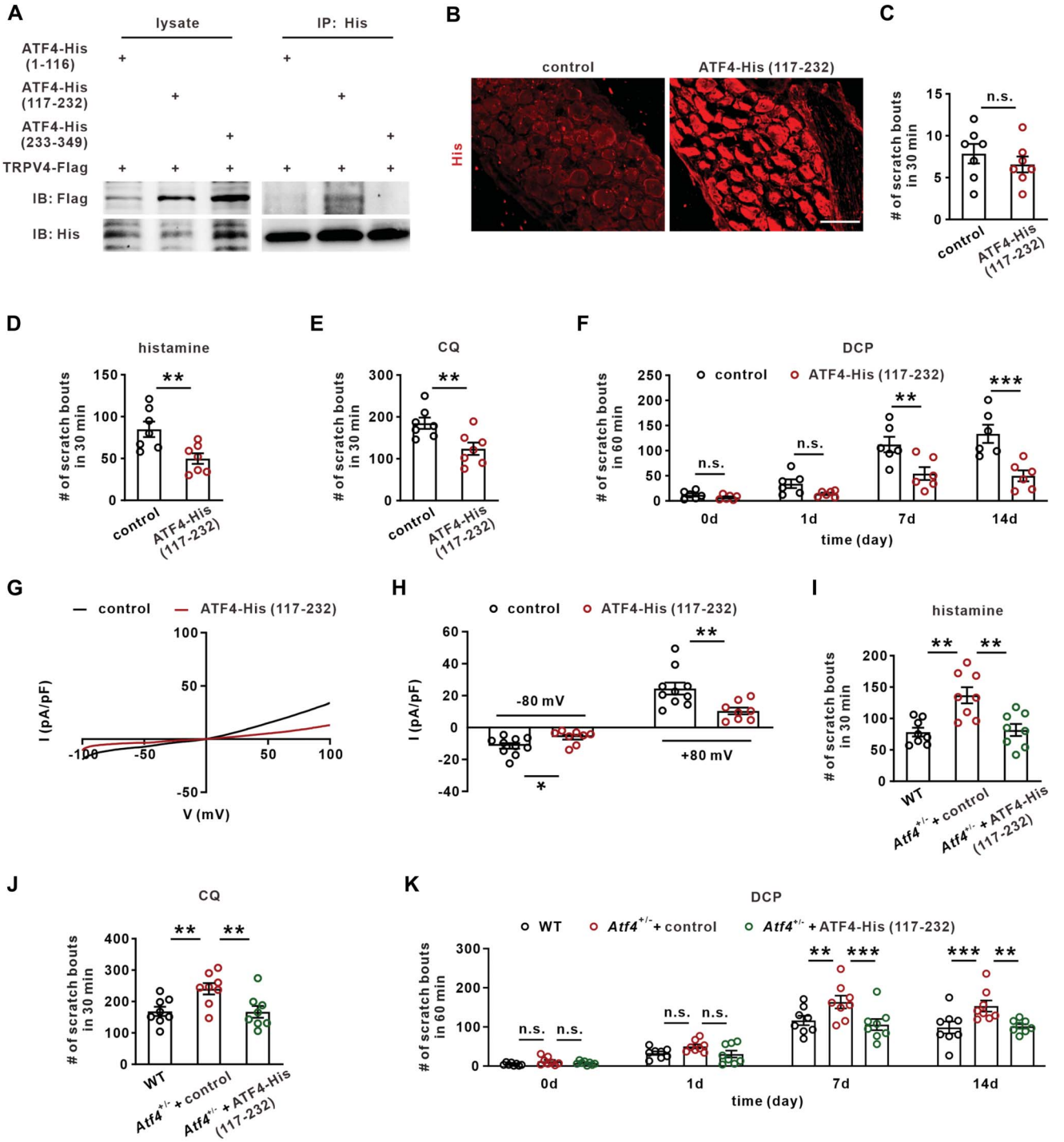

Figure 8. ATF4 regulates the function of TRPV4 through 117-232aa fragments. (A) Interaction between TRPV4 and ATF4 fragments. The ATF4-His (1-116 aa), ATF4-His (117-232 aa), and ATF4-His (233-349 aa) were transiently coexpressed with TRPV4, and the cell lysates were immunoprecipitated with antibodies as indicated. This experiment was repeated 3 times. (B) The expression of ATF4-His (117-232) fragments in DRGs of mice after intrathecal injection with rAAV-hSyn-*Atf4-His (117-232)*-2A-EGFP in 21 days. Scale bar, 100 μm. (C) The effect of intrathecal injecting rAAV-hSyn-*Atf4-His (117-232)*-2A-EGFP on the spontaneous scratching behaviors of mice. n = 7 mice per group. (D and E) The effect of intrathecal injection of rAAV-hSyn-*Atf4-His (117-232)*-2A-EGFP on the acute itch induced by histamine and CQ. n = 7 mice per group. (F) The effect of intrathecal injecting rAAV-hSyn-*Atf4-His (117-232)* -2A-EGFP on the chronic itch induced by DCP. n = 6 mice per group. (G and H) The effect of intrathecal injection of rAAV-hSyn-*Atf4-His (117-232)*-2A-EGFP on the TRPV4 current induced by 4-αPDD (TRPV4 agonist, 10 μM) in sensory neurons. n = 8 to 10 neurons per group. (I–K) The effect of intrathecal injection of rAAV-hSyn-*Atf4-His (117-232)*-2A-EGFP on the acute and chronic itch in *Atf4*$^{+/-}$ mice. n = 8 mice per group. (C–E, H) Two-tailed independent Student *t* test; (F and K), 2-way ANOVA followed by Bonferroni multiple comparisons test; (I, J), One-way ANOVA followed by Tukey multiple comparisons test; *$P < 0.05$, **$P < 0.01$, ***$P < 0.001$, n.s, means not significant. The error bars indicate the SEMs. ANOVA, analysis of variance; ATF4, activated transcription factor 4; CQ, chloroquine; DCP, diphenylcyclopropenone; DRG, dorsal root ganglion; TRPV4, transient receptor potential cation channel subfamily V member 4; 4-αPDD, 4α-Phorbol-12,13-didecanoate.

scratching behaviors both in mice and nonhuman primates, indicating that ATF4 may function as a general negative regulator in itch regulation. To confirm this, further research on additional itch models is required. Overexpression of ATF4 in sensory neurons markedly alleviates the acute and chronic pruritus. Consistent with the behavioral phenotype, using in vivo calcium

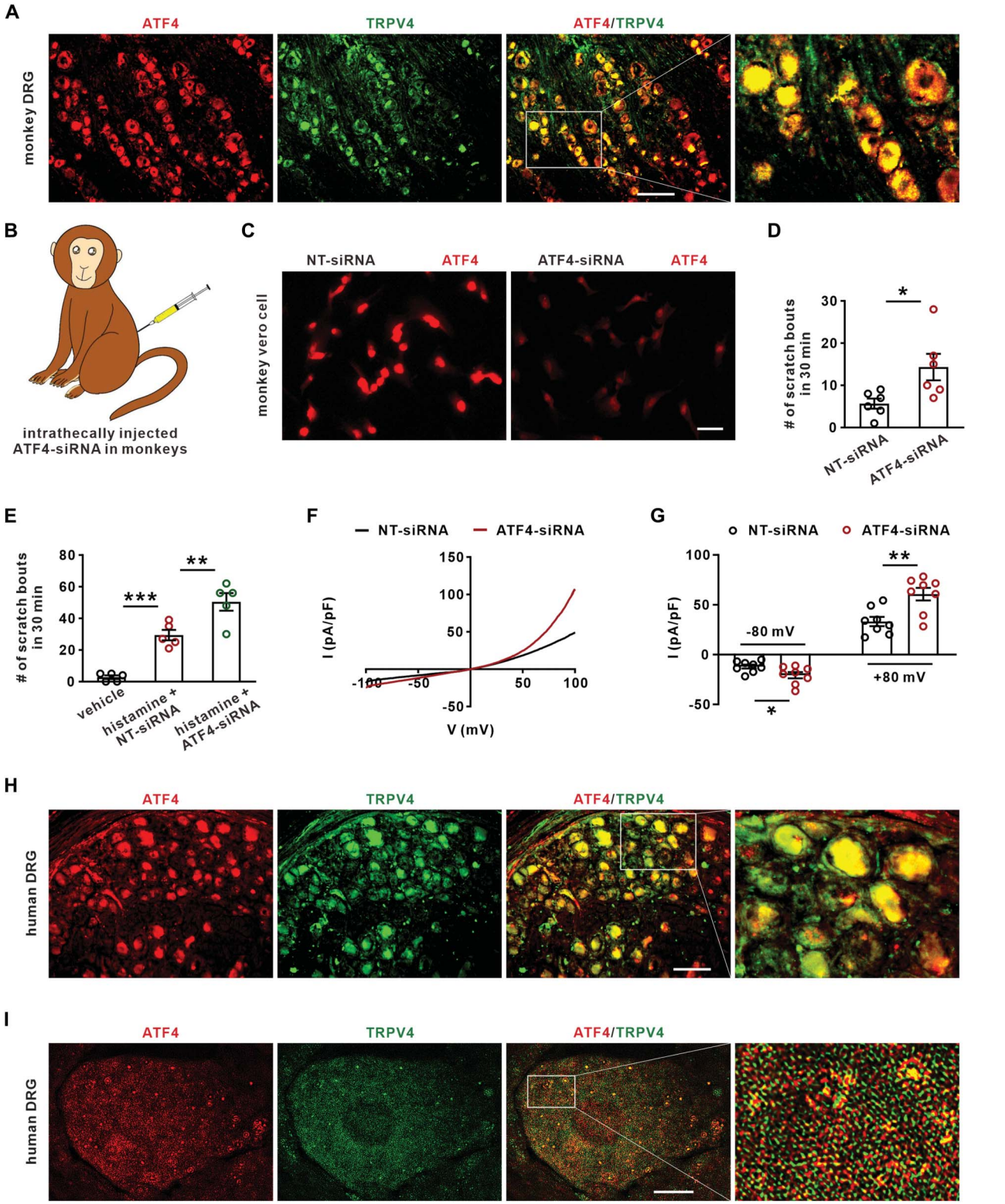

Figure 9. Interference with ATF4 increases acute itch sensitivity in nonhuman primates, and ATF4 colocalizes with TRPV4 in human sensory neurons. (A) Double immunostaining of ATF4 and TRPV4 in DRG sections of monkeys. Scale bar, 200 μm. (B) Monkeys were administered ATF4-siRNA through intrathecal (i.t.) injection, and then, the experiments were performed after 2 days. (C) Immunostaining shows the expression of ATF4 by ATF4-siRNA treatment (50 nM, 48 hours) in monkey vero cells. Scale bar, 50 μm. (D) The effect of intrathecal injection of ATF4-siRNA on the spontaneous scratching behaviors in monkeys. n = 6 monkeys per group. (E) Intrathecal injection of ATF4-siRNA on the acute itch induced by histamine in monkeys. n = 5 monkeys per group. (F and G) The effect of ATF4-siRNA on the TRPV4 current induced by 4-αPDD (TRPV4 agonist, 10 μM) in sensory neurons of monkey. n = 8 neurons per group. (H) Double immunostaining of ATF4 and TRPV4 in DRG sections of humans. Scale bar, 200 μm. (I) The high-resolution images show that the colocalization between ATF4 and TRPV4 in DRG neurons of humans. Scale bar, 10 μm. (D and G) Two-tailed independent Student *t* test; (E), 1-way ANOVA followed by Tukey multiple comparisons test. $^{*}P < 0.05$, $^{**}P < 0.01$, $^{***}P < 0.001$, n.s, means not significant. The error bars indicate the SEMs. ANOVA, analysis of variance; ATF4, activated transcription factor 4; DRG, dorsal root ganglion; TRPV4, transient receptor potential cation channel subfamily V member 4; 4-αPDD, 4α-Phorbol-12,13-didecanoate.

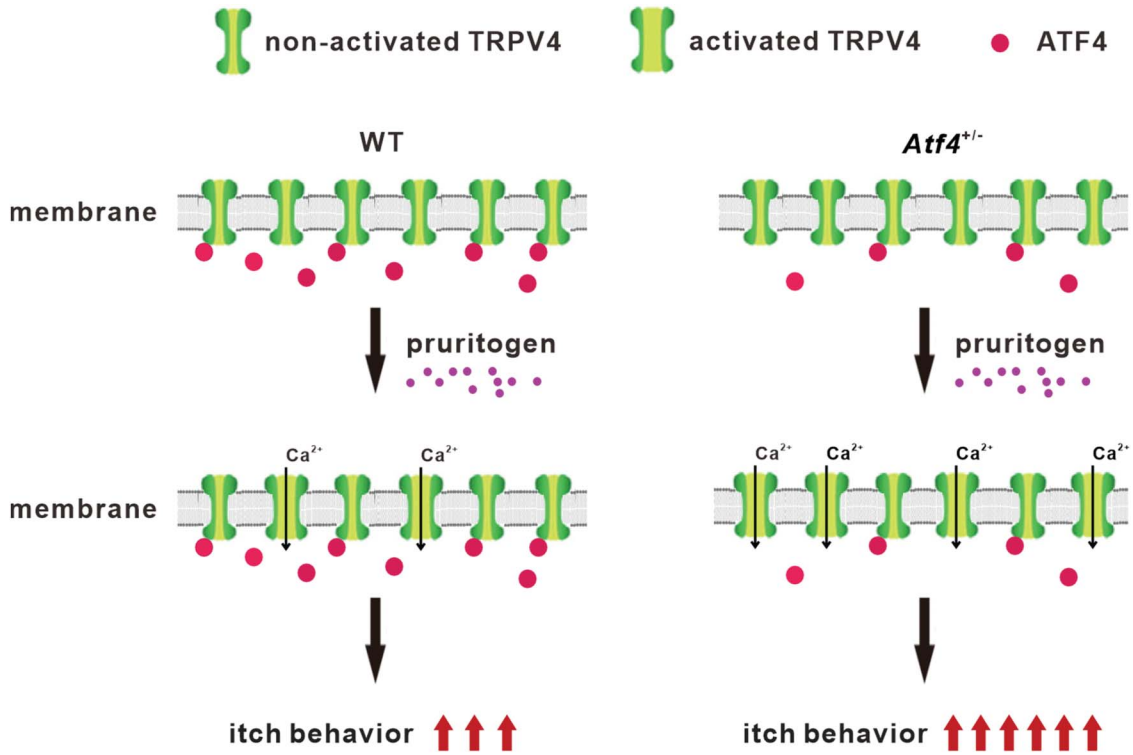

Figure 10. Hypothetical model illustrating that ATF4 interacts with TRPV4 to inhibit the function of TRPV4 in sensory neurons, and a lack of ATF4 increases TRPV4 current and promotes itch behavior. ATF4, activated transcription factor 4; TRPV4, transient receptor potential cation channel subfamily V member 4.

imaging of populations of DRG neurons, we reveal an enhanced response (in both small-sized and medium-sized cells) to the stimuli with histamine and CQ in *Atf4*$^{+/-}$ mice, indicating that ATF4 controls the itch behavior by regulating the activity of sensory neurons. Although a greater number of neurons are activated by histamine and CQ in *Atf4*$^{+/-}$ mice, it remains unclear, which specific neuronal subpopulation is being additionally activated, necessitating further research to address this issue. In summary, ATF4 may be a potential target for a variety of diseases, including AD, pathological pain, and chronic pruritus.

Transient receptor potential cation channel subfamily V member 4 is a nonselective cation channel that is abundant in sensory neurons and plays a key role in the sensory modulation of itch signals.[1,33] Study has shown that complete deletion of TRPV4 significantly inhibit histamine-induced and chloroquine (CQ)-induced acute pruritus behavior in mice.[33] Mutation of TRPV4 also markedly alleviates chronic pruritus resulting from dry skin induced by an acetone/ether mixture followed by water (AEW) and allergic contact dermatitis induced by squaric acid dibutylester (SADBE).[40] Our data presented indicate that ATF4 interacts with TRPV4. Intriguingly, the deletion of ATF4 does not alter the membrane, cytoplasmic, or total expression of TRPV4, yet it notably increases the currents of TRPV4 in DRG neurons. This unexpected discovery implies that ATF4, functioning as a transcription factor, does not regulate TRPV4 through gene expression but rather exerts a direct inhibitory effect on TRPV4 function by binding to it. This unveils a novel dimension to the regulatory mechanisms between ATF4 and TRPV4 in DRG neurons. This may be an important function of transcription factors in addition to transcription, but further studies are needed. Currently, the exploration of the nontranscriptional functions of transcription factors represents a pivotal area of research. As widely recognized, nuclear factor-kappa B (NF-κB) serves as a classical transcription factor that regulates the structure and function of the nervous system through transcription.[46,54] Our recent work shows that NF-κB interacts with Nav1.7 in sensory neurons to enhance the current density of Nav1.7 and contributes to neuropathic pain in a nontranscriptional manner.[65] Although ATF4 is a transcription factor, it also has functions other than transcription. Previous studies have shown that ATF4 directly interacts with $GABA_B$ receptors in the soma and the dendritic membrane surface of both hippocampal neurons and retinal amacrine cells.45,50,60 Our previous research has shown that knocking down ATF4 significantly diminishes the membrane expression of TRPM3 channels without affecting the total expression of TRPM3 in DRG neurons. This indicates that ATF4 governs the membrane trafficking of TRPM3 channels through a nontranscriptional mechanism.[64] Therefore, ATF4, despite its role as a transcription factor, may also participate in nontranscriptional regulatory processes. Our data show that ATF4 interacts with TRPV4 through the 117-232 aa fragments and overexpression of the ATF4 117-232 aa fragments significantly remits the histamine-evoked and CQ-evoked acute pruritus and DCP-evoked chronic pruritus in mice. These suggest that the synthesis of ATF4 117-232 aa peptide can be used as a potential drug for clinical treatment of pruritus, which needs further study. Because ATF4 plays a crucial role in the regulation of multiple physiological functions and direct intervention of ATF4 expression may result in multiple side effects, the development of ATF4 117-232 aa small peptide drug is of great clinical significance.

Our data showed that ATF4 is involved in the regulation of SLIGRL-induced acute itch and DNFB-induced allergic contact dermatitis chronic itch. Study has shown that knocking out TRPV4 in Nav1.8 positive sensory neurons has no effect on SLIGRL-induced acute itch and DNFB-induced allergic dermatitis chronic itch.[69] This suggests that the regulatory mechanism of ATF4 on SLIGRL-induced and DNFB-induced itch may not involve the modulation of TRPV4 but potentially operates through alternative

pathways. The research indicates that SLIGRL and DNFB induce itching through the modulation of Mas-related G protein–coupled receptors (Mrgprs).[38,68] Both our study and research by colleagues reveal that ATF4 participates in regulating the membrane trafficking of ion channels and receptors in neurons.[11,64] It remains unclear whether ATF4 is involved in the regulation of SLIGRL-induced and DNFB-induced itch by modulating Mrgprs membrane trafficking. Further research is needed to elucidate this mechanism. In addition to the itch regulation, TRPV4 also plays a significant role in modulating neuropathic pain[9,28] and mechanotransduction in muscle fiber afferents.[20] Moreover, TRPV4 exhibits widespread expression in brain neurons, serving as a potential risk factor for the development of brain diseases,[36] including cerebral ischemic reperfusion injury,[29] brain edema,[39] intracerebral hemorrhage,[52] epilepsy,[62] and Parkinson disease.[35] Thus, the function of TRPV4 in the body is broad, rather than itch specific. Our data indicate that ATF4 regulates a broader spectrum of itch types compared with TRPV4. This suggests that ATF4 exhibits diverse potential mechanisms in controlling itching. The inhibitory effect of ATF4 on TRPV4 might represent just one aspect of its modulation of the itch mechanism. However, to confirm this, more extensive and in-depth research is required. Although single-cell sequencing results indicate that TRPV4 is primarily expressed in C-touch fibers that are not responsive to pruritogens,[34] numerous studies have confirmed its involvement in regulating itch, such as histamine, 48/80, 5-HT, AEW, and so on.[1,33,69,70] However, there are also studies indicating that TRPV4 does not play a role in regulating itching induced by SLIGRL and DNFB.[69] Therefore, the next focus of research should be to determine the types of itching in which TRPV4 is involved in regulation and those in which it is not.

In summary, we focused on 2 main aspects. First, we investigated the regulatory role of ATF4 in itch, suggesting that ATF4 may be a potential target for itch therapy. Second, we explored the interaction between ATF4 and TRPV4 proteins, as well as ATF4's nontranscriptional regulation of TRPV4, revealing potential mechanisms through which ATF4 regulates itch.

Conflict of interest statement

The authors have no conflict of interest to declare.

Acknowledgments

This study was supported by National Natural Science Foundation of China (82271241 and 82001172 to X.L.Z., 82171230 to M.X.X.). Guangdong Basic and Applied Basic Research Foundation (2022A1515012389 to M.X.X.). Young Talent Support Project of Guangzhou Association for Science and Technology (QT20220101169 to X.L.Z.). Excellent Young Talents Project of Guangdong Provincial People's Hospital, Guangdong Academy of Medical Sciences (KY012021188 to X.L.Z.). National Research Institute for Family Planning (2021KYSHX01501 to H.H.S.). National Key R&D Program of China (2018YFC2001805 to H.H.S.).

M.-X.X., J.-H.R., X.-Y.T., and J.-K.L. contributed equally to this work. X.-L.Z. and H.-H.S. are joint corresponding authors.

Data availability statement: Requests for materials and data should be addressed to X.-L.Z. (Email: zhangxiaolong@gdph.org.cn).

Appendix A. Supplemental digital content

Supplemental digital content associated with this article can be found online at http://links.lww.com/PAIN/C9.

Article history:
Received 30 May 2023
Received in revised form 14 December 2023
Accepted 3 January 2024
Available online 28 February 2024

References

[1] Akiyama T, Ivanov M, Nagamine M, Davoodi A, Carstens MI, Ikoma A, Cevikbas F, Kempkes C, Buddenkotte J, Steinhoff M, Carstens E. Involvement of TRPV4 in serotonin-evoked scratching. J Invest Dermatol 2016;136:154–60.
[2] Andersen HH, Lo Vecchio S, Gazerani P, Arendt-Nielsen L. Dose-response study of topical allyl isothiocyanate (mustard oil) as a human surrogate model of pain, hyperalgesia, and neurogenic inflammation. PAIN 2017;158:1723–32.
[3] Baleriola J, Walker CA, Jean YY, Crary JF, Troy CM, Nagy PL, Hengst U. Axonally synthesized ATF4 transmits a neurodegenerative signal across brain regions. Cell 2014;158:1159–72.
[4] Bandell M, Macpherson LJ, Patapoutian A. From chills to chilis: mechanisms for thermosensation and chemesthesis via thermoTRPs. Curr Opin Neurobiol 2007;17:490–7.
[5] Basbaum AI, Bautista DM, Scherrer G, Julius D. Cellular and molecular mechanisms of pain. Cell 2009;139:267–84.
[6] Bautista DM, Wilson SR, Hoon MA. Why we scratch an itch: the molecules, cells and circuits of itch. Nat Neurosci 2014;17:175–82.
[7] Bell JK, McQueen DS, Rees JL. Involvement of histamine H4 and H1 receptors in scratching induced by histamine receptor agonists in Balb C mice. Br J Pharmacol 2004;142:374–80.
[8] Chen A, Muzzio IA, Malleret G, Bartsch D, Verbitsky M, Pavlidis P, Yonan AL, Vronskaya S, Grody MB, Cepeda I, Gilliam TC, Kandel ER. Inducible enhancement of memory storage and synaptic plasticity in transgenic mice expressing an inhibitor of ATF4 (CREB-2) and C/EBP proteins. Neuron 2003;39:655–69.
[9] Chen Y, Kanju P, Fang Q, Lee SH, Parekh PK, Lee W, Moore C, Brenner D, Gereau RW IV, Wang F, Liedtke W. TRPV4 is necessary for trigeminal irritant pain and functions as a cellular formalin receptor. PAIN 2014;155:2662–72.
[10] Clapham DE. TRP channels as cellular sensors. Nature 2003;426:517–24.
[11] Corona C, Pasini S, Liu J, Amar F, Greene LA, Shelanski ML. Activating transcription factor 4 (ATF4) regulates neuronal activity by controlling GABABR trafficking. J Neurosci 2018;38:6102–13.
[12] Costa-Mattioli M, Gobert D, Stern E, Gamache K, Colina R, Cuello C, Sossin W, Kaufman R, Pelletier J, Rosenblum K, Krnjevic K, Lacaille JC, Nader K, Sonenberg N. eIF2alpha phosphorylation bidirectionally regulates the switch from short- to long-term synaptic plasticity and memory. Cell 2007;129:195–206.
[13] Dawes JM, Weir GA, Middleton SJ, Patel R, Chisholm KI, Pettingill P, Peck LJ, Sheridan J, Shakir A, Jacobson L, Gutierrez-Mecinas M, Galino J, Walcher J, Kuhnemund J, Kuehn H, Sanna MD, Lang B, Clark AJ, Themistocleous AC, Iwagaki N, West SJ, Werynska K, Carroll L, Trendafilova T, Menassa DA, Giannoccaro MP, Coutinho E, Cervellini I, Tewari D, Buckley C, Leite MI, Wildner H, Zeilhofer HU, Peles E, Todd AJ, McMahon SB, Dickenson AH, Lewin GR, Vincent A, Bennett DL. Immune or genetic-mediated disruption of CASPR2 causes pain hypersensitivity due to enhanced primary afferent excitability. Neuron 2018;97:806–22.e10.
[14] Dong L, Guarino BB, Jordan-Sciutto KL, Winkelstein BA. Activating transcription factor 4, a mediator of the integrated stress response, is increased in the dorsal root ganglia following painful facet joint distraction. Neuroscience 2011;193:377–86.
[15] Donnelly CR, Jiang C, Andriessen AS, Wang K, Wang Z, Ding H, Zhao J, Luo X, Lee MS, Lei YL, Maixner W, Ko MC, Ji RR. STING controls nociception via type I interferon signalling in sensory neurons. Nature 2021;591:275–80.
[16] Ebert SM, Monteys AM, Fox DK, Bongers KS, Shields BE, Malmberg SE, Davidson BL, Suneja M, Adams CM. The transcription factor ATF4 promotes skeletal myofiber atrophy during fasting. Mol Endocrinol 2010;24:790–9.
[17] Elefteriou F, Benson MD, Sowa H, Starbuck M, Liu X, Ron D, Parada LF, Karsenty G. ATF4 mediation of NF1 functions in osteoblast reveals a nutritional basis for congenital skeletal dysplasiae. Cell Metab 2006;4:441–51.
[18] Everaerts W, Zhen X, Ghosh D, Vriens J, Gevaert T, Gilbert JP, Hayward NJ, McNamara CR, Xue F, Moran MM, Strassmaier T, Uykal E, Owsianik

G, Vennekens R, De Ridder D, Nilius B, Fanger CM, Voets T. Inhibition of the cation channel TRPV4 improves bladder function in mice and rats with cyclophosphamide-induced cystitis. Proc Natl Acad Sci U S A 2010;107:19084–9.
[19] Feng J, Luo J, Yang P, Du J, Kim BS, Hu H. Piezo2 channel-Merkel cell signaling modulates the conversion of touch to itch. Science 2018;360:530–3.
[20] Fukazawa A, Hori A, Hotta N, Katanosaka K, Estrada JA, Ishizawa R, Kim HK, Iwamoto GA, Smith SA, Vongpatanasin W, Mizuno M. Antagonism of TRPV4 channels partially reduces mechanotransduction in rat skeletal muscle afferents. J Physiol 2023;601:1407–24.
[21] Gao X, Han S, Huang Q, He SQ, Ford NC, Zheng Q, Chen Z, Yu S, Dong X, Guan Y. Calcium imaging in population of dorsal root ganglion neurons unravels novel mechanisms of visceral pain sensitization and referred somatic hypersensitivity. PAIN 2021;162:1068–81.
[22] Grant AD, Cottrell GS, Amadesi S, Trevisani M, Nicoletti P, Materazzi S, Altier C, Cenac N, Zamponi GW, Bautista-Cruz F, Lopez CB, Joseph EK, Levine JD, Liedtke W, Vanner S, Vergnolle N, Geppetti P, Bunnett NW. Protease-activated receptor 2 sensitizes the transient receptor potential vanilloid 4 ion channel to cause mechanical hyperalgesia in mice. J Physiol 2007;578:715–33.
[23] Hai T, Curran T. Cross-family dimerization of transcription factors Fos/Jun and ATF/CREB alters DNA binding specificity. Proc Natl Acad Sci U S A 1991;88:3720–4.
[24] Han J, Back SH, Hur J, Lin YH, Gildersleeve R, Shan J, Yuan CL, Krokowski D, Wang S, Hatzoglou M, Kilberg MS, Sartor MA, Kaufman RJ. ER-stress-induced transcriptional regulation increases protein synthesis leading to cell death. Nat Cell Biol 2013;15:481–90.
[25] Han Q, Liu D, Convertino M, Wang Z, Jiang C, Kim YH, Luo X, Zhang X, Nackley A, Dokholyan NV, Ji RR. miRNA-711 binds and activates TRPA1 extracellularly to evoke acute and chronic pruritus. Neuron 2018;99:449–63.e6.
[26] Han SK, Simon MI. Intracellular signaling and the origins of the sensations of itch and pain. Sci Signaling 2011;4:er3.
[27] He CH, Gong P, Hu B, Stewart D, Choi ME, Choi AM, Alam J. Identification of activating transcription factor 4 (ATF4) as an Nrf2-interacting protein. Implication for heme oxygenase-1 gene regulation. J Biol Chem 2001;276:20858–65.
[28] Hu X, Du L, Liu S, Lan Z, Zang K, Feng J, Zhao Y, Yang X, Xie Z, Wang PL, Ver Heul AM, Chen L, Samineni VK, Wang YQ, Lavine KJ, Gereau RW IV, Wu GF, Hu H. A TRPV4-dependent neuroimmune axis in the spinal cord promotes neuropathic pain. J Clin Invest 2023;133:e161507.
[29] Jie P, Lu Z, Hong Z, Li L, Zhou L, Li Y, Zhou R, Zhou Y, Du Y, Chen L, Chen L. Activation of transient receptor potential vanilloid 4 is involved in neuronal injury in middle cerebral artery occlusion in mice. Mol Neurobiol 2016;53:8–17.
[30] Johanek LM, Meyer RA, Friedman RM, Greenquist KW, Shim B, Borzan J, Hartke T, LaMotte RH, Ringkamp M. A role for polymodal C-fiber afferents in nonhistaminergic itch. J Neurosci 2008;28:7659–69.
[31] Kanehisa K, Koga K, Maejima S, Shiraishi Y, Asai K, Shiratori-Hayashi M, Xiao MF, Sakamoto H, Worley PF, Tsuda M. Neuronal pentraxin 2 is required for facilitating excitatory synaptic inputs onto spinal neurons involved in pruriceptive transmission in a model of chronic itch. Nat Commun 2022;13:2367.
[32] Karin M, Smeal T. Control of transcription factors by signal transduction pathways: the beginning of the end. Trends Biochemical Sciences 1992;17:418–22.
[33] Kim S, Barry DM, Liu XY, Yin S, Munanairi A, Meng QT, Cheng W, Mo P, Wan L, Liu SB, Ratnayake K, Zhao ZQ, Gautam N, Zheng J, Karunarathne WK, Chen ZF. Facilitation of TRPV4 by TRPV1 is required for itch transmission in some sensory neuron populations. Sci Signaling 2016;9:ra71.
[34] Li CL, Li KC, Wu D, Chen Y, Luo H, Zhao JR, Wang SS, Sun MM, Lu YJ, Zhong YQ, Hu XY, Hou R, Zhou BB, Bao L, Xiao HS, Zhang X. Somatosensory neuron types identified by high-coverage single-cell RNA-sequencing and functional heterogeneity. Cell Res 2016;26:83–102.
[35] Liu N, Bai L, Lu Z, Gu R, Zhao D, Yan F, Bai J. TRPV4 contributes to ER stress and inflammation: implications for Parkinson's disease. J Neuroinflammation 2022;19:26.
[36] Liu N, Wu J, Chen Y, Zhao J. Channels that cooperate with TRPV4 in the brain. J Mol Neurosci 2020;70:1812–20.
[37] Liu Q, Tang Z, Surdenikova L, Kim S, Patel KN, Kim A, Ru F, Guan Y, Weng HJ, Geng Y, Undem BJ, Kollarik M, Chen ZF, Anderson DJ, Dong X. Sensory neuron-specific GPCR Mrgprs are itch receptors mediating chloroquine-induced pruritus. Cell 2009;139:1353–65.
[38] Liu Q, Weng HJ, Patel KN, Tang Z, Bai H, Steinhoff M, Dong X. The distinct roles of two GPCRs, MrgprC11 and PAR2, in itch and hyperalgesia. Sci Signaling 2011;4:ra45.
[39] Lu KT, Huang TC, Tsai YH, Yang YL. Transient receptor potential vanilloid type 4 channels mediate Na-K-Cl-co-transporter-induced brain edema after traumatic brain injury. J Neurochem 2017;140:718–27.
[40] Luo J, Feng J, Yu G, Yang P, Mack MR, Du J, Yu W, Qian A, Zhang Y, Liu S, Yin S, Xu A, Cheng J, Liu Q, O'Neil RG, Xia Y, Ma L, Carlton SM, Kim BS, Renner K, Liu Q, Hu H. Transient receptor potential vanilloid 4-expressing macrophages and keratinocytes contribute differentially to allergic and nonallergic chronic itch. J Allergy Clin Immunol 2018;141:608–19.e7.
[41] Masuoka HC, Townes TM. Targeted disruption of the activating transcription factor 4 gene results in severe fetal anemia in mice. Blood 2002;99:736–45.
[42] Meixiong J, Anderson M, Limjunyawong N, Sabbagh MF, Hu E, Mack MR, Oetjen LK, Wang F, Kim BS, Dong X. Activation of mast-cell-expressed mas-related G-protein-coupled receptors drives non-histaminergic itch. Immunity 2019;50:1163–71.e5.
[43] Misery L, Brenaut E, Pierre O, Le Garrec R, Gouin O, Lebonvallet N, Abasq-Thomas C, Talagas M, Le Gall-Ianotto C, Besner-Morin C, Fluhr JW, Leven C. Chronic itch: emerging treatments following new research concepts. Br J Pharmacol 2021;178:4775–91.
[44] Moore C, Gupta R, Jordt SE, Chen Y, Liedtke WB. Regulation of pain and itch by TRP channels. Neurosci Bull 2018;34:120–42.
[45] Nehring RB, Horikawa HP, El Far O, Kneussel M, Brandstatter JH, Stamm S, Wischmeyer E, Betz H, Karschin A. The metabotropic GABAB receptor directly interacts with the activating transcription factor 4. J Biol Chem 2000;275:35185–91.
[46] Niederberger E, Geisslinger G. The IKK-NF-kappaB pathway: a source for novel molecular drug targets in pain therapy? FASEB J 2008;22:3432–42.
[47] Ohno M. Roles of eIF2α kinases in the pathogenesis of Alzheimer's disease. Front Mol Neurosci 2014;7:22.
[48] Pasini S, Corona C, Liu J, Greene LA, Shelanski ML. Specific downregulation of hippocampal ATF4 reveals a necessary role in synaptic plasticity and memory. Cell Rep 2015;11:183–91.
[49] Pathak SS, Liu D, Li T, de Zavalia N, Zhu L, Li J, Karthikeyan R, Alain T, Liu AC, Storch KF, Kaufman RJ, Jin VX, Amir S, Sonenberg N, Cao R. The eIF2α kinase GCN2 modulates period and rhythmicity of the circadian clock by translational control of Atf4. Neuron 2019;104:724–35.e6.
[50] Ritter B, Zschuntsch J, Kvachnina E, Zhang W, Ponimaskin EG. The GABA(B) receptor subunits R1 and R2 interact differentially with the activation transcription factor ATF4 in mouse brain during the postnatal development. Brain Res Develop Brain Res 2004;149:73–7.
[51] Rutkowski DT, Kaufman RJ. All roads lead to ATF4. Develop Cell 2003;4:442–4.
[52] Shen J, Tu L, Chen D, Tan T, Wang Y, Wang S. TRPV4 channels stimulate Ca(2+)-induced Ca(2+) release in mouse neurons and trigger endoplasmic reticulum stress after intracerebral hemorrhage. Brain Res Bull 2019;146:143–52.
[53] Siu F, Bain PJ, LeBlanc-Chaffin R, Chen H, Kilberg MS. ATF4 is a mediator of the nutrient-sensing response pathway that activates the human asparagine synthetase gene. J Biol Chem 2002;277:24120–7.
[54] Srinivasan M, Lahiri DK. Significance of NF-κB as a pivotal therapeutic target in the neurodegenerative pathologies of Alzheimer's disease and multiple sclerosis. Expert Opin Ther Targets 2015;19:471–87.
[55] Sun YG, Zhao ZQ, Meng XL, Yin J, Liu XY, Chen ZF. Cellular basis of itch sensation. Science 2009;325:1531–4.
[56] Sutaria N, Adawi W, Goldberg R, Roh YS, Choi J, Kwatra SG. Itch: pathogenesis and treatment. J Am Acad Dermatol 2022;86:17–34.
[57] Tanaka T, Tsujimura T, Takeda K, Sugihara A, Maekawa A, Terada N, Yoshida N, Akira S. Targeted disruption of ATF4 discloses its essential role in the formation of eye lens fibres. Genes Cells 1998;3:801–10.
[58] van der Steen PH, van Baar HM, Perret CM, Happle R. Treatment of alopecia areata with diphenylcyclopropenone. J Am Acad Dermatol 1991;24:253–7.
[59] Vandewauw I, Owsianik G, Voets T. Systematic and quantitative mRNA expression analysis of TRP channel genes at the single trigeminal and dorsal root ganglion level in mouse. BMC Neurosci 2013;14:21.
[60] Vernon E, Meyer G, Pickard L, Dev K, Molnar E, Collingridge GL, Henley JM. GABA(B) receptors couple directly to the transcription factor ATF4. Mol Cell Neurosci 2001;17:637–45.
[61] Wang Z, Jiang C, He Q, Matsuda M, Han Q, Wang K, Bang S, Ding H, Ko MC, Ji RR. Anti-PD-1 treatment impairs opioid antinociception in rodents and nonhuman primates. Sci Transl Med 2020;12:eaaw6471.
[62] Wang Z, Zhou L, An D, Xu W, Wu C, Sha S, Li Y, Zhu Y, Chen A, Du Y, Chen L, Chen L. TRPV4-induced inflammatory response is involved in

neuronal death in pilocarpine model of temporal lobe epilepsy in mice. Cell Death Dis 2019;10:386.
[63] Wortel IMN, van der Meer LT, Kilberg MS, van Leeuwen FN. Surviving stress: modulation of ATF4-mediated stress responses in normal and malignant cells. Trends Endocrinol Metab 2017;28:794–806.
[64] Xie MX, Cao XY, Zeng WA, Lai RC, Guo L, Wang JC, Xiao YB, Zhang X, Chen D, Liu XG, Zhang XL. ATF4 selectively regulates heat nociception and contributes to kinesin-mediated TRPM3 trafficking. Nat Commun 2021;12:1401.
[65] Xie MX, Zhang XL, Xu J, Zeng WA, Li D, Xu T, Pang RP, Ma K, Liu XG. Nuclear factor-kappaB gates Nav1.7 channels in DRG neurons via protein-protein interaction. iScience 2019;19:623–33.
[66] Xing Y, Chen J, Hilley H, Steele H, Yang J, Han L. Molecular signature of pruriceptive MrgprA3(+) neurons. J Invest Dermatol 2020;140:2041–50.
[67] Yan J, Ye F, Ju Y, Wang D, Chen J, Zhang X, Yin Z, Wang C, Yang Y, Zhu C, Zhou Y, Cao P, Xu Y, Yu G, Tang Z. Cimifugin relieves pruritus in psoriasis by inhibiting TRPV4. Cell Calcium 2021;97:102429.
[68] Yang N, Shao H, Deng J, Yang Y, Tang Z, Wu G, Liu Y. Dictamnine ameliorates chronic itch in DNFB-induced atopic dermatitis mice via inhibiting MrgprA3. Biochem Pharmacol 2023;208:115368.
[69] Zhang Q, Dias F, Fang Q, Henry G, Wang Z, Suttle A, Chen Y. Involvement of sensory neurone-TRPV4 in acute and chronic itch behaviours. Acta Dermato Venereol 2022;102:adv00651.
[70] Zhang Q, Henry G, Chen Y. Emerging role of transient receptor potential vanilloid 4 (TRPV4) ion channel in acute and chronic itch. Int J Mol Sci 2021;22:7591.
[71] Zimmermann M. Ethical guidelines for investigations of experimental pain in conscious animals. PAIN 1983;16:109–10.